

Invited Review

Gamma-Ray Line Emission from Radioactive Isotopes in Stars and Galaxies

ROLAND DIEHL

Max-Planck-Institut für extraterrestrische Physik, Giessenbachstrasse 1, D-85740 Garching, Germany; rod@mpe-garching.mpg.de

AND

F. X. TIMMES

Center for Astrophysics and Space Sciences University of California at San Diego, La Jolla, CA 92093; and Institute for Theoretical Physics, University of California at Santa Barbara, Santa Barbara, CA 93106; fxt@burn.uchicago.edu

Received 1997 October 29; accepted 1998 January 26

ABSTRACT. Our modern laboratory of nuclear physics has expanded to encompass parts of the universe, or at least our Galaxy. Gamma rays emitted by the decays of radioactive nuclei testify to the production of isotopes through nuclear processes in astrophysical events. We collect measurements of the Galactic γ -ray sky in spectral lines attributed to the decay of radioactive ${}^7\text{Be}$, ${}^{22}\text{Na}$, ${}^{26}\text{Al}$, ${}^{44}\text{Ti}$, ${}^{56}\text{Ni}$, ${}^{57}\text{Ni}$, and ${}^{60}\text{Fe}$. We organize and collate these measurements with models for the production sites in novae, supernovae, stellar interiors, and interstellar cosmic-ray interactions. We discuss the physical processes and the spatial distribution of these production sites, along with models of the chemical evolution of the Galaxy. Highlights of measurements made in the last decade include detailed images of the Galaxy in ${}^{26}\text{Al}$ radioactivity and detection of ${}^{56}\text{Co}$ and ${}^{57}\text{Co}$ from SN 1987A, ${}^{44}\text{Ti}$ from Cas A, and possibly ${}^{56}\text{Ni}$ from SN 1991T. The ${}^{26}\text{Al}$ mapping of recent Galactic nucleosynthesis may be considered as a new view on the entire ensemble of massive stars in the Galaxy. The local Cygnus region shows prominent radioactive emission from well-known stellar clusters, but the absence of γ -rays from the closest Wolf-Rayet star, WR 11, in the Vela region is puzzling. SN 1987A studies in γ -rays measure the radioactive powering of the supernova light curve directly, which will be particularly important for the dim late phase powered by ${}^{44}\text{Ti}$. The ${}^{57}\text{Ni}/{}^{56}\text{Ni}$ isotopic ratio determinations from γ -rays provide additional guidance for understanding SN 1987A's complex light curve and now appear to be uniformly settling to about twice the solar ratio. Cas A ${}^{44}\text{Ti}$ production as measured through γ -rays presents the interesting puzzle of hiding the expected, coproduced, and large ${}^{56}\text{Ni}$ radioactivity. Core-collapse supernova models need to parameterize the inner boundary conditions of the supernova in one way or another, and now enjoy another measurement of the ejecta that is definitely originating from very close to the difficult regime of the mass cut between ejecta and compact remnant. Other relevant measurements of cosmic element abundances, such as observations of atomic lines from the outer shells of the production sites or meteoritic analysis of interstellar grains, complement the rather direct measurements of penetrating γ -rays, thus enhancing the observational constraints of nuclear astrophysics models.

1. INTRODUCTION

Radioactivity was discovered a little more than a century ago when Henri Becquerel included potassium and uranium sulfates as part of a photographic emulsion mixture (Becquerel 1896). He soon found that all uranium compounds and the metal itself were “light sources,” with an intensity proportional to the amount of uranium present; the chemical combination had no effect. Two years later, Pierre and Marie Curie coined the term “radioactive” for those elements that emitted such “Becquerel rays.” A year later, Ernest Rutherford demonstrated that at least three different kinds of radiation are emitted in the decay of radioactive substances. He called these “alpha,” “beta,” and “gamma” rays in an increasing order of their ability to penetrate matter (Rutherford 1899; Feather 1973). It took a few more years for Rutherford and others to conclusively show

that the alpha rays were identical with the nuclei of helium atoms (Rutherford 1905; Rona 1978), and that the beta rays were electrons (Becquerel 1900; Badash 1979). By 1912 it was shown that the γ -rays had all the properties of very energetic electromagnetic radiation (see, e.g., Allen 1911), but a full appreciation of the physics underlying the measurements took another two decades (Compton 1929).

We now understand radioactive decay as transitions between different states of atomic nuclei, transitions that are ultimately attributed to electroweak interactions. Measurement of the decay products has grown into an important tool of experimental physics. On Earth, it forms the basis of radioactive dating through high-precision isotopic analysis, in tree rings, terrestrial rocks, and meteoritic samples, to name just a few examples (Rolfs & Rodney 1989). Radioactive material throughout the

distant universe may be studied in detail by measuring the material's γ -ray line spectrum. These γ -ray lines identify a specific isotope, and the abundance of the distant material directly relates to the measured γ -ray line intensity (Clayton 1982). These γ -rays are also unaffected by the intervening matter once the radioactive nucleus has left its dense production site and gone into the interstellar medium. The characteristic half-life of an isotope constitutes an exposure timescale of the sky in a specific γ -ray line. Given reasonable event frequencies and stellar nucleosynthesis yields, the cumulative radioactivity from many events (^{26}Al , ^{60}Fe , and to a lesser extent ^{22}Na and ^{44}Ti), and individual events (^{44}Ti , ^{56}Ni , ^{57}Ni , and perhaps ^7Be , ^{22}Na) can be examined.

By the late 1970s various international collaborations had launched experiments on stratospheric balloons and space satellites to explore cosmic rays and X-ray, and γ -ray sources (Murthy & Wolfendale 1993). The first γ -ray line found was reported by Haymes et al. (1975), and their discovery triggered 20 years of often controversial measurements and interpretations of positron annihilation radiation studies. Several additional lines were discovered shortly thereafter, including the *HEAO C* measurement of line γ -rays from $\sim 2\text{--}3 M_{\odot}$ of the trace isotope ^{26}Al from the central region of the Galaxy (Mahoney et al. 1982). After those pioneering missions provided new measurements with tantalizing implications, the *Compton Gamma Ray Observatory (CGRO)* was launched in 1991 April to explore the γ -ray sky for the first time over a wide range of γ -ray energies, including the regime of nuclear lines from radioactivity. A delightful summary of the *CGRO*'s history and relationship to the previous missions, by Kniffen, Gehrels, & Fishman (1998), complements the description of the *CGRO*'s goals, instrumentation, and first achievements by Gehrels et al. (1993). Today, collaborative international agencies have numerous ongoing and planned projects to deepen specific studies in the area of γ -ray astronomy (see, e.g., Winkler et al. 1997; Kurfess et al. 1998).

In the following review, attention is chiefly focused on the Milky Way's γ -ray line emission that originates from the radioactive isotopes ^7Be , ^{22}Na , ^{26}Al , ^{44}Ti , ^{56}Ni , ^{57}Ni , and ^{60}Fe . The reviews by Lingenfelter & Ramaty (1978) and Ramaty & Lingenfelter (1995) provide excellent supplementary material.

2. PRODUCTION OF RADIOACTIVE ISOTOPES

The nucleosynthetic processes in stars responsible for the production of ^{26}Al have been summarized by Clayton & Leising (1987), Prantzos & Diehl (1996), and MacPherson, Davis, & Zinner (1995). In stars, ^{26}Al is produced by proton capture reactions, mainly on ^{25}Mg , and is destroyed by e^+ decay and (n, p) , (n, α) , and (p, γ) reactions. The final yield from any source is temperature sensitive. ^{26}Al can be produced during (1) hydrostatic hydrogen burning in the core of massive ($\geq 11 M_{\odot}$) stars; (2) hydrostatic hydrogen burning in the hydrogen shell of low- and intermediate-mass ($\leq 9 M_{\odot}$) stars while on

the asymptotic giant branch; (3) explosive hydrogen burning (temperatures $> 2 \times 10^8 \text{ K}$) in massive stars and on the surfaces of white dwarfs (i.e., novae); and (4) hydrostatic and explosive carbon and neon burning in massive stars. Any ^{26}Al produced by stars is ejected in part by strong winds (Wolf-Rayet, asymptotic giant branch stars) and in full amount by explosions (supernova and nova). Besides being formed in stars, ^{26}Al can also in principle be produced by spallation reactions of high-energy cosmic rays on a range of nuclei (mainly silicon, aluminum, and magnesium), although at substantially lower efficiency. In fact, ^{26}Al has recently been reported discovered in cosmic-ray composition studies with the *Ulysses* spacecraft (Simpson & Connell 1998).

Once produced, ^{26}Al decays with a half-life of $7.5 \times 10^5 \text{ yr}$ from its $J^{\pi} = 5^+$ ground state by β^+ -decay (82% of the time) and e^- capture to the $J^{\pi} = 2^+$ excited state of ^{26}Mg . This excited state then falls to the $J^{\pi} = 0^+$ ground state of ^{26}Mg , emitting a 1.809 MeV γ -ray photon.

Most of the different ways to synthesize ^{26}Al —Type II supernovae, Wolf-Rayet stars, AGB stars, and classical novae—can, at least according to their respective proponents, produce sufficient quantities Galaxy-wide. But they cannot all make the advertised amounts, or else there would be too much ^{26}Al in the Galaxy. Each prospective source has its advantages and difficulties. We discuss their nature briefly, addressing a few of the physical aspects involved.

The treatment of convection, and its implications, constitute one problem area common to several source types. The convective coupling between mass zones in both the oxygen-neon and hydrogen shell-burning regions of massive stars can simultaneously bring light reactants and seed nuclei into the hot zone to aid in the synthesis, and through the same process remove the fragile product from the high-temperature region where it might otherwise be destroyed. Convective burning in the oxygen-neon shell of a $20 M_{\odot}$ star has been modeled in two dimensions by Bazan & Arnett (1994). They find that large-scale plume structures dominate the velocity field, physically caused by the inertia contained in moving mass cells. As a result, significant mixing beyond the boundaries defined conventionally by mixing-length theory brings fresh fuel into the convective region ("convective overshoot"), which may cause local hot spots of nuclear burning. This is different from the situation encountered in spherically symmetric computations. We will have to await improvements in those very resource-demanding calculations to assess the inadequacies of mixing-length theory and its application in the detailed one-dimensional models currently defining the baseline. Chemical inhomogeneities create gradients of chemical composition, which provide yet another driver of mixing ("semiconvection"). Large-scale mass motions and local burning conditions are likely to change the quantitative yields of many isotopes from any single massive star. However, any nonmonotonic and/or stochastic nature of the nucleosynthetic yields as a function of stellar mass tends to be smoothed out by integration over a

stellar population, with its initial mass function contributing to the observable γ -ray emission. Thus, the general features of the integrated yields, as determined from spherically symmetric models, may remain a useful approximation.

Rotation may also have large systematic effects. In massive stars, the amount of mixing in the hydrogen envelope is increased, thus processing more ^{25}Mg into ^{26}Al . The helium core mass may be larger as a result, thus leading to more ^{26}Al in the larger neon-oxygen layers (Meynet & Maeder 1997; Langer et al. 1997). Rotating or not, complete loss of the hydrogen and helium layers, either through mass loss as a single star or through the effects of close binary evolution (Braun & Langer 1995), could affect the quantitative yields of most of the pre-supernova abundances. Recent improvement of the physical ingredients in Wolf-Rayet ^{26}Al production models provides some consolidation of hydrostatic nucleosynthesis in massive stars (Arnould, Paulus, & Meynet 1997; Meynet et al. 1997). These studies point out that combinations of metallicity and mass loss can increase the ejected mass of ^{26}Al by ~ 2 . The ^{26}Al abundance present in the hydrogen shell is ejected unmodified in the supernova explosion or, in more massive stars during their Wolf-Rayet phase, by a stellar wind.

The ^{26}Al synthesized in the oxygen-neon shell may be significantly enhanced because of operation of the neutrino process (Woosley et al. 1990). Protons liberated by ν spallation of ^{20}Ne capture on ^{25}Mg to produce ^{26}Al . When the oxygen-neon shells are located closer to the collapsing core, a higher ν flux is encountered. This may enhance the ^{26}Al yield by $\sim 50\%$. The relative importance of the ν process contribution depends on the ν energy spectrum. The peak μ and τ neutrino temperature in real supernovae is somewhat uncertain (Myra & Burrows 1990), in spite of measurements from SN 1987A (Arnett et al. 1989). Few transport calculations have been carried out long enough (at least 3 s) and with sufficient energy resolution to see the hardening of the neutrino spectrum that occurs as the proto-neutron star cools (although see Burrows, Hayes, & Fryxell 1995; Mezzacappa et al. 1998). Nevertheless, these uncertainties should be seen in perspective: Nuclear reaction uncertainties are substantial on the $^{25}\text{Mg}(p, \gamma)$ production reaction as well as on the destructions through $^{26}\text{Al}(p, \gamma)$, in addition the rapidly decaying ^{26}Al state at 228 keV excitation energy becomes an important agent in oxygen burning.

The genesis of the central compact remnant in core-collapse supernovae bears on several interesting physical problems, some of which may be constrained by radioactivity observations. Formation of a neutron star appears likely for main-sequence masses below $\sim 19 M_{\odot}$, while a black hole probably forms for main-sequence masses above this regime (Timmes, Woosley, & Weaver 1996b; Woosley & Timmes 1996). The energy of the explosion, placement of the mass cut, and how much mass falls back onto the remnant shortly after the explosion, all modify this neutron star-black hole bifurcation point. Each of these processes also affects the mass of nucleosynthetic products ejected from the inner regions of the su-

pernova. For example, producing more than $10^{-4} M_{\odot}$ of radioactive ^{44}Ti is difficult in spherically symmetric models that are exploded with a piston, but making much less in such models is easy. Ejection of *any* ^{44}Ti is especially sensitive to how much mass falls back onto the remnant. To achieve a nearly constant kinetic energy of the ejecta (as supernova remnant observations suggest), the explosion energy in $M \geq 25 M_{\odot}$ presupernova models must be steadily increased in order to overcome the increased binding energy of the mantle. However, even in the 35 and 40 M_{\odot} stars the presupernova density profile may still cause nearly all the produced ^{44}Ti to fall back onto the compact remnant. Unless the explosion mechanism, for unknown reasons, provides a much larger characteristic energy in more massive stars, it appears likely that stars larger than about 30 M_{\odot} will have dramatically reduced ^{44}Ti yields and leave massive remnants ($M \geq 10 M_{\odot}$) that become black holes. If, however, the explosion is energetic enough (perhaps overly energetic) more ^{44}Ti is ejected. Rotation may modify this picture significantly by breaking the spherical symmetry of the explosion. Jets that are enriched in ^{44}Ti may be induced in the polar regions and still remain in agreement with energy arguments given above (Nagataki et al. 1997).

The origin and evolution of an accreting white dwarf that becomes a classical novae is essentially unknown, yet has important consequences on any γ -ray signal that may originate from novae. For example, the composition of the nuclear burning region is often assumed to be a 50-50 mixture of accreted material and dredged-up white dwarf material. Typically, the accreted material is taken to have a solar composition, and the white dwarf material is assumed to be an oxygen-neon-magnesium mixture in mass proportions of 0.3 : 0.5 : 0.2 (see, e.g., Politano et al. 1995). Recent evolutionary models of a 10 M_{\odot} star (Ritossa, Garcia-Berro, & Iben 1996), however, suggest that oxygen-neon-magnesium ratios of 0.5 : 0.3 : 0.05 might be more appropriate, although the detailed abundances could vary substantially with initial stellar mass. Since the yields of ^{26}Al and ^{22}Na from nova are sensitive to the initial ^{25}Mg and ^{20}Ne abundances, if this latter white dwarf composition is confirmed, then it eliminates most of the necessary seed material from which radioactive isotopes may be synthesized. Uncertainty in binary star evolution and the binary mass distribution function correspond to uncertainty in the fraction of classical novae that originate from $\geq 8 M_{\odot}$ main-sequence stars (Kolb & Politano 1997). Finally, all nova models predict ejected masses that are too small by an order of magnitude when compared with observations (see, e.g., Hernanz et al. 1996). As the white dwarf becomes more massive, less material is accreted before the fuel ignites, and the total mass of matter lifted to escape velocity, ^{22}Na and ^{26}Al in particular, is smaller. If the inconsistency between model and observed ejected masses is resolved by resorting to a less massive ($M \leq 1.1 M_{\odot}$) white dwarf, then the ^{26}Al yields are expected to increase owing to the lower burning temperatures (José, Hernanz, & Coc 1997). However, should a more violent explosion be required, and be

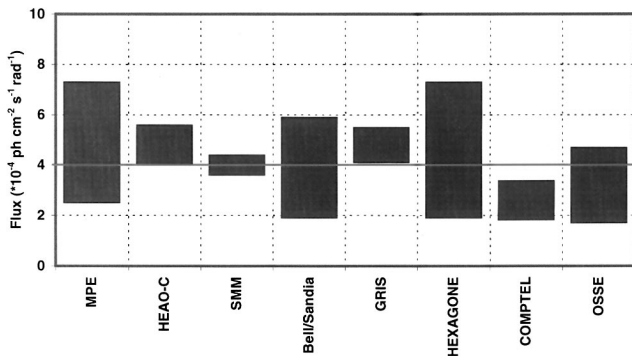


FIG. 1.—Reported 1.809 MeV flux values for the inner Galaxy, from eight experiments. The length of each vertical stripe is set by the reported uncertainties. A value of $\sim 4 \times 10^{-4}$ photons $\text{cm}^{-2} \text{s}^{-1} \text{rad}^{-1}$ appears plausible given all experiments, although some discrepancies will have to be investigated (adapted from Diehl et al. 1998).

achieved by increased mixing of core material, then the higher burning temperatures are expected to decrease the ^{26}Al mass ejected. While these examples show that our understanding of the physics is rather incomplete, the thermonuclear runaway model for classical novae has been a first-order success. A novae event within 1 kpc would provide several important diagnostics (radioactive and otherwise) for refining the mixing and energetics aspects of the model.

Gamma-ray astronomy seeks to constrain the astrophysical origin site(s) of radioactive isotopes in the Galaxy, and on smaller spatial scales, regions of coherent star formation. Sometimes the dominant origin site (supernovae, novae, Wolf-Rayet stars, AGB stars, cosmic rays) of a Galactic radioactivity are not immediately clear from the observations, but are valuable to know. The differences between any derived spatial distributions of the competing sources are often not large enough to provide a crisp discriminant, especially since young population stars relate to several of the source types (Prantzos & Diehl 1996). Increasing the resolution to subdegree domains should provide a better test of various questions (e.g., do AGB stars give a 1.809 MeV glow that trails the spiral arms?), but that option must await the next generation of γ -ray telescopes. Are there other measurable quantities that might help distinguish between competing sources? One method is to look for correlated productions with other radioactive isotopes. For example, γ -rays from radioactive ^{60}Fe may be a very good discriminant for the contested origin site of Galactic ^{26}Al for two main reasons: (1) Type II supernovae produce comparable amounts of ^{26}Al and ^{60}Fe , while the other potential candidates produce significantly smaller amounts of ^{60}Fe . (2) Even more important, the “ ^{26}Al follows ^{60}Fe ” model can be tested with present generation γ -ray spectrometers. For individual events, other physical parameters are often observed in great detail, so the general nature of the origin site is usually clear. In these individual events γ -ray line measurements can provide specific constraints in themselves, or complement any constraints ob-

tained otherwise. We will discuss γ -ray line emission from radioactive isotopes on Galactic scales and from individual sources in the following.

3. INTEGRATED NUCLEOSYNTHESIS

The *High-Energy Astronomical Observatory C (HEAO C)* discovery of the 1.809 MeV γ -ray line from radioactive ^{26}Al in the Galaxy (Mahoney et al. 1982), which had been anticipated from theoretical considerations (Clayton 1971, 1982; Arnett 1977; Ramaty & Lingenfelter 1977; Lingenfelter & Ramaty 1978), opened new doors in γ -ray astronomy. Measurements of various radioactive decays in the Milky Way offer a global proof of the idea that heavy-element formation is an ongoing process and is still happening inside stars (Burbidge et al. 1957; Cameron 1957). In particular, radioactive decay times of $\sim 10^6$ yr (as for ^{26}Al and ^{60}Fe) probe a timescale that is short compared to galactic evolution, thus testifying to the occurrence of relatively recent nucleosynthesis events throughout the Galaxy. The ^{26}Al and ^{60}Fe isotopes provide this unique observational window, since massive-star nucleosynthesis is expected to produce these trace elements in quantities sufficient to yield γ -ray line fluxes above instrumental threshold sensitivities. For typical yields of $\sim 10^{-4} M_{\odot}$ per event, approximately 10,000 individual events will contribute to the line emission from the Galaxy, typical fluxes of degree-sized source regions are $\sim 10^{-5}$ photons $\text{cm}^{-2} \text{s}^{-1}$.

3.1. ^{26}Al in the Galaxy

Eight experiments over the 15 years since its discovery by *HEAO C* (Mahoney et al. 1982) have reported detecting γ -ray emission from radioactive ^{26}Al (see review by Prantzos & Diehl 1996). Instrumental capabilities differ substantially, but the integrated flux measured from the general direction of the inner Galaxy, integrated over latitude and the inner radian in longitude, has been used to roughly compare results. We summarize the flux values in Figure 1, including the results reviewed by Prantzos & Diehl (1996) plus the recent Gamma-Ray Imaging Spectrometer (GRIS) measurement (Naya et al. 1996). All measurements are consistent with values $\sim 4 \times 10^{-4}$ photons $\text{cm}^{-2} \text{s}^{-1} \text{rad}^{-1}$, as indicated by the horizontal line. Note that the determination method varies between the instruments, and in particular the flux values for the nonimaging instruments depend on the assumed spatial distribution: All nonimaging instruments essentially assume the same (or equivalent) smooth spatial distribution narrowly following the plane of the Galaxy as it had been derived from *COS B* measurements of Galactic γ -rays in the 100 MeV regime. The distribution of 1.809 MeV emission seems significantly different, however. Maximum entropy deconvolution images derived from measurements by the Compton Telescope (COMPTEL) aboard the *CGRO* show spatial structure in the emission (Fig. 2). The ridge of the Galactic plane dominates, but there is asymmetry in the emission profile along the disk, and there are several prominent regions of emis-

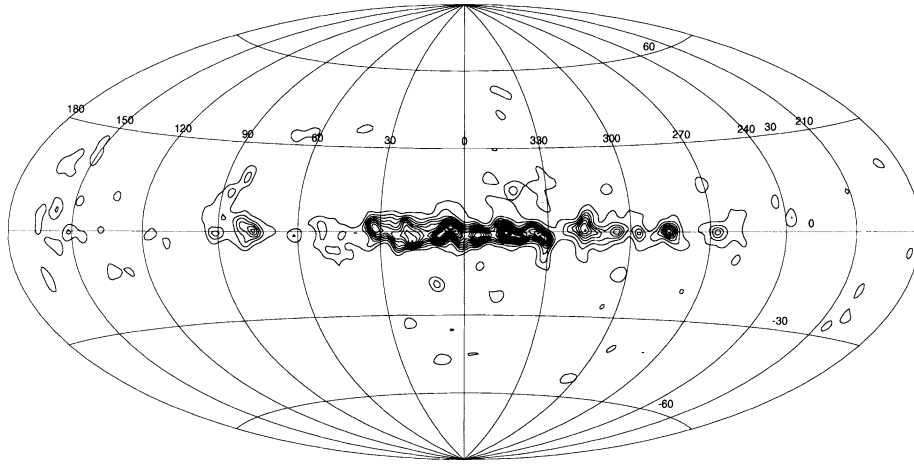


FIG. 2.—COMPTEL 1.8 MeV all-sky image, derived from 5 yr of observation through maximum entropy deconvolution (adapted from Oberlack 1998)

sion such as Vela and Cygnus. All estimates of the absolute ^{26}Al mass in the Galaxy rest on assumptions about the spatial distribution of the sources, since the 1.809 MeV measurements themselves do not carry distance information. The COMPTEL team fitted a wide range of models for candidate source spatial distributions to their data. When localized regions of emission beyond the inner Galaxy are excluded, then all axisymmetric model fits yield a Galactic mass of $\approx 2 M_{\odot}$ (Diehl et al. 1995; Knödlseher et al. 1996a; Diehl et al. 1998). The extent of spiral-arm emission can be estimated if a composite model of disk emission plus emission along spiral arms is adopted and compared with the disk-only model. Spiral structure appears significant, including between $1.1 M_{\odot}$ and all of the ^{26}Al (Diehl et al. 1997; Knödlseher et al. 1996a).

If massive stars are the candidate sources, they were thought to follow the molecular gas distribution, and thus would be represented by CO survey data (Dame et al. 1987). Although generally compatible with the ^{26}Al map, other tracers were found to provide a better fit. One of these tracers is a semi-analytical model of spiral-arm structure based on H II region data but refined by free-electron measurements from pulsar signal dispersions. This tracer shows ridges similar to the ^{26}Al map at longitudes $\pm 35^{\circ}$, along with a prominent feature in Carina ($l = 280^{\circ}$), which supports the connection to a young stellar population (Taylor & Cordes 1993; Chen et al. 1997).

This indicates that tracers which measure the energy input into the interstellar medium from massive stars appear to be an approximate representation of the ^{26}Al source distribution. Examples are warm dust maps such as the long-wavelength *Cosmic Background Explorer* (COBE) DIRBE maps, or the far-infrared cooling lines of the ionized interstellar medium (e.g., C^+) (Diehl et al. 1998). In a recent multifrequency image comparison it was demonstrated that a map of the ionization power from massive stars (free-free emission) as derived from the COBE DMR map (after correction for the synchrotron con-

tribution) is proportional to the 1.809 MeV map in all significant detail over the entire plane of the Galaxy (Knödlseher 1998). Assuming a standard initial mass function, this calculation reproduces the expected massive-star population and the supernova rate from both maps consistently, if Wolf-Rayet stars from high-metallicity regimes in the inner Galaxy provide the bulk of ^{26}Al (Knödlseher 1998).

The evidence above may be taken to constrain ^{26}Al contributions from classical novae, where a smooth distribution of the emission with a pronounced peak in the central bulge region would be expected. The upper limit for such contributions is probably $1 M_{\odot}$ of ^{26}Al . On the other hand, Ne-rich novae in our Galaxy may occur more frequently in the disk and hence follow the Galactic distribution of massive stars more closely than the overall white dwarf distribution. In this case, differentiating nova sources from massive-star sources will rely on the consistency of the calculated yields with other lines of evidence (such as another radioactive isotope), assisted by 1.809 MeV line-shape arguments.

From the apparent (yet not very significant) ^{26}Al flux inconsistencies visible in Figure 1, studies of more local ^{26}Al contributions have been revived: The low value from COMPTEL is mainly based on Galactic plane emission, while the large field-of-view instruments (100° – 160°) of GRIS and *Solar Maximum Mission* (SMM) mainly sampled the sky along the plane of the ecliptic with relatively more exposure of the high-latitude sky; those instruments may capture large-scale flux of low surface brightness that COMPTEL's image failed to capture. ^{26}Al emission from the solar vicinity had been predicted long ago (see, e.g., Morfill & Hartquist 1985; Blake & Dearborn 1989) but was discarded when COMPTEL's image had shown dominating emission along the plane of the Galaxy. Local contributions to the overall emission may exist: the existence of two pulsars at ~ 100 pc distances (Geminga and R CrA), but also the nearby Gould Belt structure dominated by B stars, and

massive-star activity signposts such as Loop I, attributed to the nearby Sco-Cen association, suggest that the ~ 500 pc environment of the Sun may well have experienced a higher than average star formation and supernova activity since ~ 50 million years ago (see, e.g., Pöppel 1997). In view of the very different instrumental techniques, each with substantial systematic uncertainties, the flux measurements must be consolidated and ensured to be comparable, before such speculations are pursued.

Imaging of MeV γ -rays is far from straightforward because of the high instrumental backgrounds and the complex γ -ray detection methods. Consistency checks between different techniques have shown that some of the spikiness of the apparent emission in the COMPTEL result can be an artifact of analysis techniques (see, e.g., Knödlseider 1998). Nevertheless, significant emission from the Cygnus, Carina, and Vela regions appears consolidated. In the Vela region, there was some hope to detect ^{26}Al from one single source, the nearby Vela supernova remnant (Oberlack et al. 1994; Diehl et al. 1995). Recent results show, however, that the main 1.809 MeV feature is significantly offset from the Vela supernova remnant. The offset may be caused by emission superimposed from a newly discovered young supernova remnant, and/or by OB associations and shell-like features at larger distances (Oberlack 1998). A direct calibration of core-collapse supernova nucleosynthesis, which was a tantalizing prospect 2 years ago (Diehl et al. 1995), does not appear as feasible. The other prominent candidate source in the Vela region is the binary system γ^2 Velorum, representing the Wolf-Rayet star WR 11 closest to the Sun with an O star companion (van der Hucht et al. 1988). Recent *Hipparcos* parallax measurements suggest that this binary system is at a distance of 250–310 pc, which is closer than previous estimates of 300–450 pc (van der Hucht et al. 1997; Schaefer, Schmutz, & Grenon 1997). At this closer distance the absence of a signal from γ^2 Velorum in the COMPTEL 1.8 MeV data is unexpected, particularly since recent models have increased the expected ^{26}Al yields for this object (Meynet et al. 1997). Modification of the ^{26}Al ejected from WR 11 caused by the O star companion seems inadequate to account for the discrepancy (Braun & Langer 1995; Langer et al. 1997).

About 80% of the prominent 1.809 MeV emission associated with the Cygnus region can be understood in terms of the expected ^{26}Al signal from known sources (del Rio et al. 1996). One may be concerned with this high fraction, since ^{26}Al decays on a timescale longer than the observable features of supernova remnants and Wolf-Rayet winds prevail. It has been suggested that the ^{26}Al from this region attributed to “seen” sources should be multiplied by a factor of 1–10 to account for “unseen” sources. The latest COMPTEL images show structures that suggestively align with the Cygnus superbubble and Cyg OB1. Further analysis may be able to separate source regions spatially and in particular assess the significance of emission from the prominent group of Wolf-Rayet stars in this region.

The Carina region ($l = 282^\circ$ – 295°) presents a tangential view along a spiral arm, identified through a large molecular

cloud complex at ≈ 2 – 5 kpc distance (Grabelsky et al. 1987), houses the prominent $140 M_\odot$ η Carinae star ($l = 288^\circ$), and shows the densest concentration of young open clusters along the plane of the Galaxy. Knödlseider et al. (1996b) discuss that ^{26}Al production within these clusters as part of the Car OB1 association may relate to the observed 1.809 MeV feature at $l = 286^\circ$. This feature is consistent with a point source for the 4° resolution COMPTEL instrument, thus spatially more confined than the originally estimated signature from analysis of the Milky Way’s spiral structure (Prantzos 1993a, 1993b). It is also interesting that some of the 1.809 MeV image structures that fail to align with spiral arms do coincide with directions toward nearby associations of massive stars (Diehl et al. 1995; Knödlseider et al. 1998). Patchiness in such a nucleosynthetic snapshot might be expected from the clustering of formation environments of massive stars (Elmegreen & Efremov 1996). If viewed from the outside, the Milky Way might also display the signs of massive-star populations in the form of H II regions arranged like beads on a string along spiral arms, such as are observed in M31 from H α emission analysis (Williams et al. 1995) or in M51 from heated dust seen in infrared continuum at $15 \mu\text{m}$ (Kessler et al. 1996). Interstellar absorption and source confusion prevents such mapping within the Milky Way, unfortunately. Therefore, detailed investigations of the COMPTEL image systematic uncertainty, that is, a quantitative limit to artificial bumpiness of the imaging algorithm, will be important for such interpretation of 1.809 MeV emission. Such concerns also apply for other instruments and future measurements of large segments of the Galactic plane.

In a recent balloon flight, GRIS drift scanned the Galactic center region with its $\sim 100^\circ$ field of view, and detected the 1.809 MeV line at 6.8σ significance with a flux of $4.8 \pm 0.7 \times 10^{-4}$ photons $\text{cm}^{-2} \text{s}^{-1} \text{rad}^{-1}$ (Naya et al. 1996). The main surprise of this measurement is the width of the astrophysical line profile, which was significantly broader than the instrumental resolution of the germanium detector, and reported as $\Delta E = 5.4 \pm 1.4$ keV. This line width is much larger than expected from Galactic rotation (≤ 1 keV; Gehrels & Chen 1996), which dominates above the broadening from random motions in the interstellar medium (Ramaty & Lingenfelter 1977, 1995). It is presently difficult to understand how such high-velocity motion could be maintained over the million year timescale of ^{26}Al decay. Thermal broadening by a very hot phase of the interstellar medium ($\sim 10^8$ K) with long cooling times ($\sim 10^5$ yr), or a kinetic broadening at high average velocities (~ 500 km s^{-1}), seems required. Either case requires extremely low-density phases of the interstellar medium on large spatial scales (Chen et al. 1997). Alternatively, one can hypothesize massive, high-speed dust grains rich in ^{26}Al to explain the measurement (Chen et al. 1997). Further observations of the line-shape details are required to examine any spatial variations in the line broadening. Spectral resolution of ~ 2 keV is required for such a study. Although the *International Gamma-Ray Astrophysics Laboratory (INTEGRAL)* may still

have insufficient energy resolution to make complete velocity maps of the 1.809 MeV emission along the plane of the Galaxy, the brightest features can probably have their velocity centroids determined well enough to place them on the Galactic rotation curve and thus derive a distance to the features. Surveys that combine velocity information and Galactic latitude extent could then examine the existence and nature of any Galactic “fountains” and “chimneys” from possible “venting” of ^{26}Al into the Galactic halo. The COMPTEL-measured latitude width may constrain the mean velocity of observed ^{26}Al below the GRIS-suggested value for an assumed young and hence narrow population of sources and isotropic expansion over 10^6 yr (Oberlack 1998). In any case, the large line width measured by GRIS, although inconsistent with the *HEAO C* line width limit of ≤ 3 keV, needs confirmation, since it could have profound implications for our understanding of the interstellar medium in the Galaxy.

3.2. ^{60}Fe in the Galaxy

Physically, ^{60}Fe should be a good discriminant of different source types generating ^{26}Al , because massive stars produce ^{26}Al and ^{60}Fe in the same regions and in roughly comparable amounts (Fig. 3). Shown are abundances as a function of mass inside a $25 M_{\odot}$, solar metallicity, Type II supernova model (Woosley & Weaver 1995) at the end of the presupernova evolution (*dashed curve*) and the final, postexplosion abundances (*solid curves*). While the ^{26}Al production occurs in the hydrogen shell and the oxygen-neon shell, ^{60}Fe is produced in the He shell burning and at the base of the oxygen-neon shell. Most important is that the majority of both ^{26}Al and ^{60}Fe are produced, mainly during the presupernova evolution, between 3 and $6 M_{\odot}$. These two isotopes should have similar spatial distributions after the explosion of these stars.

^{26}Al and ^{60}Fe are produced in different ratios in stars of different mass (Fig. 4). Massive stars heavier than $\sim 25 M_{\odot}$ tend to synthesize more ^{26}Al than ^{60}Fe in the Woosley & Weaver (1995) models, while the two isotopes are produced in roughly equal amounts below $25 M_{\odot}$. An estimate for the injection rate into the Milky Way is the steady state event rate times the average mass ejected per event; taking $M(^{26}\text{Al}) \sim 10^{-4} M_{\odot}$, $M(^{60}\text{Fe}) \sim 4 \times 10^{-5} M_{\odot}$, and ~ 2 core-collapse supernovae per century, one has $\dot{M}(^{26}\text{Al}) \sim 2.0 M_{\odot} \text{ Myr}^{-1}$ and $\dot{M}(^{60}\text{Fe}) \sim 0.8 M_{\odot} \text{ Myr}^{-1}$. More refined chemical evolution calculations suggest that Type II supernovae are responsible for a steady state abundance of $2.2 \pm 1.1 M_{\odot}$ of ^{26}Al and $1.7 \pm 0.9 M_{\odot}$ of ^{60}Fe in the Galaxy (Timmes et al. 1995). Once ^{60}Fe can be unambiguously detected with γ -ray telescopes, we can test the hypothesis of the supernova origin of ^{26}Al , since ^{60}Fe from other sources is negligible. Thus, the ^{60}Fe flux map is then expected to follow the ^{26}Al distribution, and the $^{60}\text{Fe}/^{26}\text{Al}$ line flux ratio should be $16\% \pm 10\%$: the ^{26}Al image (see Fig. 2) will have the same morphology as the ^{60}Fe image but will be dimmer.

A few recent ^{60}Fe measurements and flux ratios with ^{26}Al

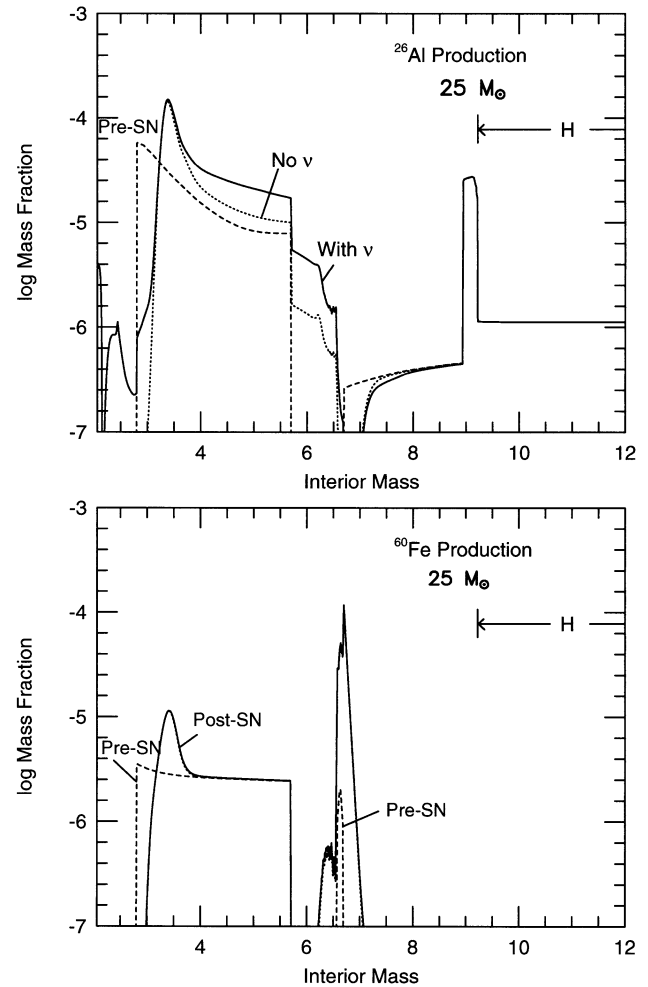


FIG. 3.—Mass profiles of ^{26}Al (top) and ^{60}Fe (bottom) for a $25 M_{\odot}$ model (adapted from Timmes et al. 1995).

are shown in Figure 4. *SMM* reported an upper limit of 8.1×10^{-5} photons $\text{cm}^{-2} \text{ s}^{-1}$ for the 1.173 MeV ^{60}Co line over the central radian of Galactic longitude, giving an upper limit of $1.7 M_{\odot}$ of ^{60}Fe (Leising & Share 1994). This ^{60}Fe mass is consistent with the expectations given above and is $\sim 20\%$ of the ^{26}Al flux. Recently, the GRIS (Naya et al. 1998), the Oriented Scintillation Spectrometer Experiment (OSSE) aboard the *CGRO* (Harris 1998), and COMPTEL (Diehl et al. 1998) teams have reported upper limit $^{60}\text{Fe}/^{26}\text{Al}$ ratios. If the stringent GRIS measurements are confirmed, then the initial model estimates for the total Galactic flux ratio might be too large. But there are uncertainties of ~ 2 in the models, from nuclear cross sections, explosion energy uncertainties (affecting the large ^{60}Fe contribution from explosive He burning), and chemical evolution models. The qualitative picture of ^{26}Al and ^{60}Fe tracing each other to a good degree of precision still presents an important observational challenge, even more so with a smaller flux ratio.

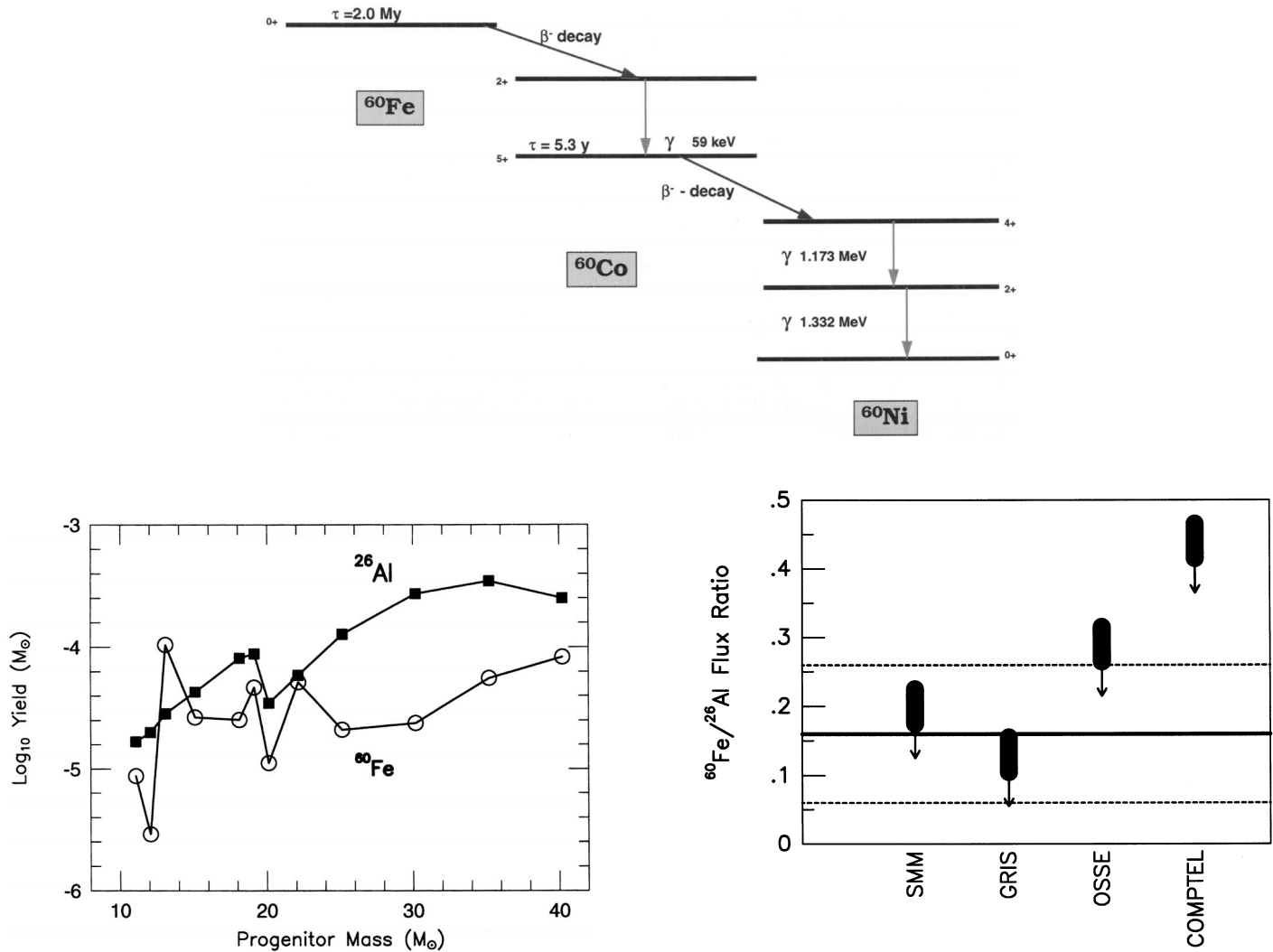


FIG. 4.—Top: Decay of ^{60}Fe showing the important spin-parity levels and γ -ray photons. Bottom left: Mass of ^{26}Al and ^{60}Fe ejected vs. main-sequence progenitor mass (adapted from Timmes et al. 1995), assuming no mass loss. Bottom right: $^{60}\text{Fe}/^{26}\text{Al}$ ratio predicted from supernova models and the preliminary ratio derived from recent measurements.

4. SHORTER LIVED RADIOACTIVITIES

4.1. ^{44}Ti

In massive stars, stable ^{44}Ca is produced chiefly, almost exclusively, as radioactive ^{44}Ti in the “ α -rich freeze-out.” This process occurs when material initially in nuclear statistical equilibrium, and a relatively low density, is cooled rapidly enough that the free α -particles do not have time to merge back into the iron group by the relatively inefficient triple- α reaction. Thus, the distribution of nuclei cools down in the presence of an anomalously large concentration of α -particles (Woosley, Arnett, & Clayton 1973; Hix & Thielemann 1996). No other ^{44}Ca production process is compatible with the large observed $^{48}\text{Ca}/^{46}\text{Ca}$ ratio. Representative yields of ^{44}Ti from solar metallicity Type II and Type Ib supernova models are shown in Figure 5 (Woosley & Weaver 1995; Woosley, Langer, &

Weaver 1995). Production in Type Ib supernovae is more uniform because the models converge to a common presupernova mass in the narrow range $2.3\text{--}3.6 M_{\odot}$. All of the models, whose ejecta all have $\sim 10^{51}$ ergs of kinetic energy at infinity, predict ^{44}Ti yields between 1 and $15 \times 10^{-5} M_{\odot}$. Typical values are $\sim 3 \times 10^{-5} M_{\odot}$ for the Type II models, or twice that value for the Type Ib models.

Thielemann, Nomoto, & Hashimoto (1996) have also examined the detailed nucleosynthesis of core-collapse supernovae, and they find, in general, that larger amounts of ^{44}Ti are ejected. The differences may be caused by how the explosion is simulated from expansion of an artificial high-entropy bubble, but partially also by the nuclear reaction rates employed, or the progenitor structure. Thielemann et al. explode their stellar models by depositing thermal energy deep in the

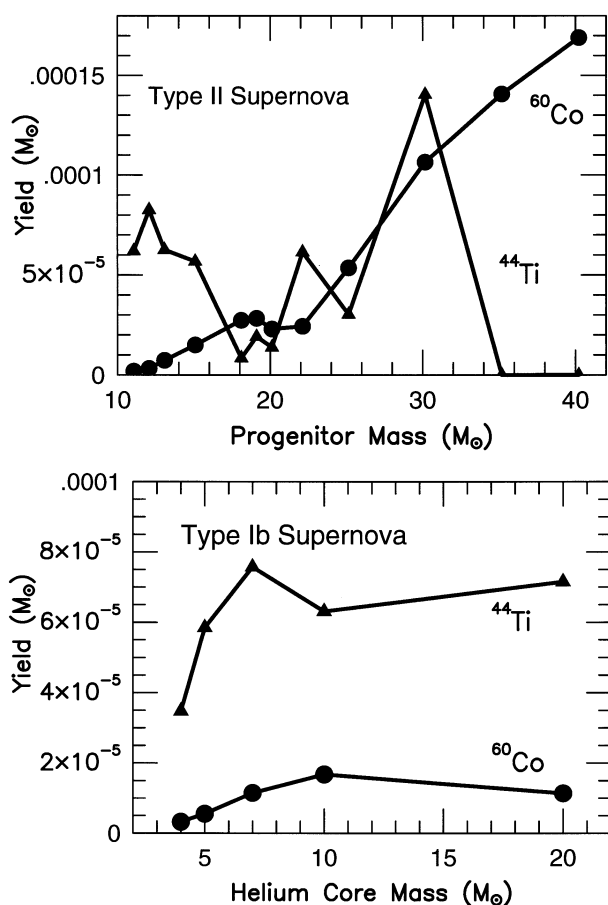


FIG. 5.— ^{44}Ti yields from Type II and Ib supernovae (adapted from Timmes et al. 1996a).

neutronized core (which later becomes the neutron star). This gives a larger entropy to the innermost zones than what a momentum- (piston)- driven explosion would impart and, in principle, eject more material. A larger entropy also ensures a more vigorous alpha-rich freeze-out, and thus a larger ^{44}Ti production. Thielemann et al. sum the ejecta from the outside of the star inward and place the mass cut (which is artificial in all models) at the position where sufficient ^{56}Ni is produced to explain the observations. Woosley & Weaver place the piston at a suitable first approximation to mass cut and then follow an explosion trajectory. It is the difference between injecting momentum or energy in modeling the explosion that leads to the two groups following different adiabatic paths (Aufderheide, Baron, & Thielemann 1991). What self-consistent explosion models do, exploding via neutrino heating and multi-dimensional convection, might be reflective of one-dimensional momentum-driven explosions, one-dimensional energy-driven explosions, or some intermediate case. Hence, the differences between the two groups in the amount of ^{44}Ti ejected is an example of the spread one obtains due to uncertainties in modeling the Type II explosion mechanism.

Asymmetries in the explosion mechanism could drive an enhancement of ^{44}Ti in the ejecta (Nagataki et al. 1997). Regions of a larger entropy material could develop behind an asymmetric shock front and incur a larger ^{44}Ti production, perhaps by as much as an order of magnitude. It is possible that core-collapse supernovae have asymmetric explosions. The high birth velocity observed for radio pulsars (Lyne & Lorimer 1994) is often taken as evidence for some small asymmetry in the explosion of core-collapse supernovae, although B -field or ν -wind asymmetry provide alternative explanations. Rotation and magnetic fields are a common characteristic of massive stars, and each could induce asymmetries. Differences in the neutrino fluxes, seeded by intermittence in the convective flows, could also drive an asymmetry. Consistent modeling of such asymmetry has not been achieved yet, and in particular the measured nickel isotope ratios provide a tight constraint on the entropy/neutron ratio in the inner nucleosynthesis region (F. Thielemann 1997, private communication).

Type Ia supernovae could also be important sources of ^{44}Ti if the sub-Chandrasekhar model turns out to be viable. Here a 0.6–0.9 M_{\odot} carbon-oxygen white dwarf accretes helium at a rate of a few times $10^{-8} M_{\odot} \text{ yr}^{-1}$ from a binary companion. (Tutukov, Yungelson, & Iben 1992; Iben & Livio 1993). When 0.15–0.20 M_{\odot} of helium has been accreted in this model, a helium detonation is initiated at the base of the accreted layer. This helium detonation compresses the carbon-oxygen core, which triggers a detonation there as well (Livne & Glasner 1991; Woosley & Weaver 1994; Livne & Arnett 1995). The broadband photometry implied by these models is generally bluer than the observed photometry of Type Ia supernovae; on the other hand, these models come closer to Type Ia spectroscopic data. The iron group nucleosynthesis is acceptable in these models, and the production factors for ^{44}Ca relative to its solar mass fraction range from 200 to 3000. Depending upon how frequently these sub-Chandrasekhar mass white dwarfs explode, the large production factors suggest that these types of thermonuclear events might be the principal origin of ^{44}Ca , rather than the typical core-collapse event. This leaves the ^{44}Ti observation from Cas A as a puzzle.

There are three γ -ray lines one can use to examine or detect the decay of ^{44}Ti ; the 67.9 and 78.4 keV lines from the ^{44}Sc de-excitation cascade and the 1.157 MeV line as ^{44}Ca decays to its stable ground state. These transitions are shown in Figure 6 with their respective spins, parities, and energies. The half-life of ^{44}Ti , used to translate observed γ -ray fluxes into a supernova mass of ^{44}Ti , has been surprisingly uncertain (Fig. 6). Measured values over the last 20 years range from 39 to 66 years, with a trend toward around 44 years for methods determining the activity, and scattering around 58 years for methods following the decay curve. The half-life is difficult to measure because the number of ^{44}Ti nuclei one can obtain is small and the half-life is large (relative to Avogadro's number and the available laboratory time, respectively). The recent measurement through the activity method with a mixed $^{44}\text{Ti}/^{22}\text{Na}$

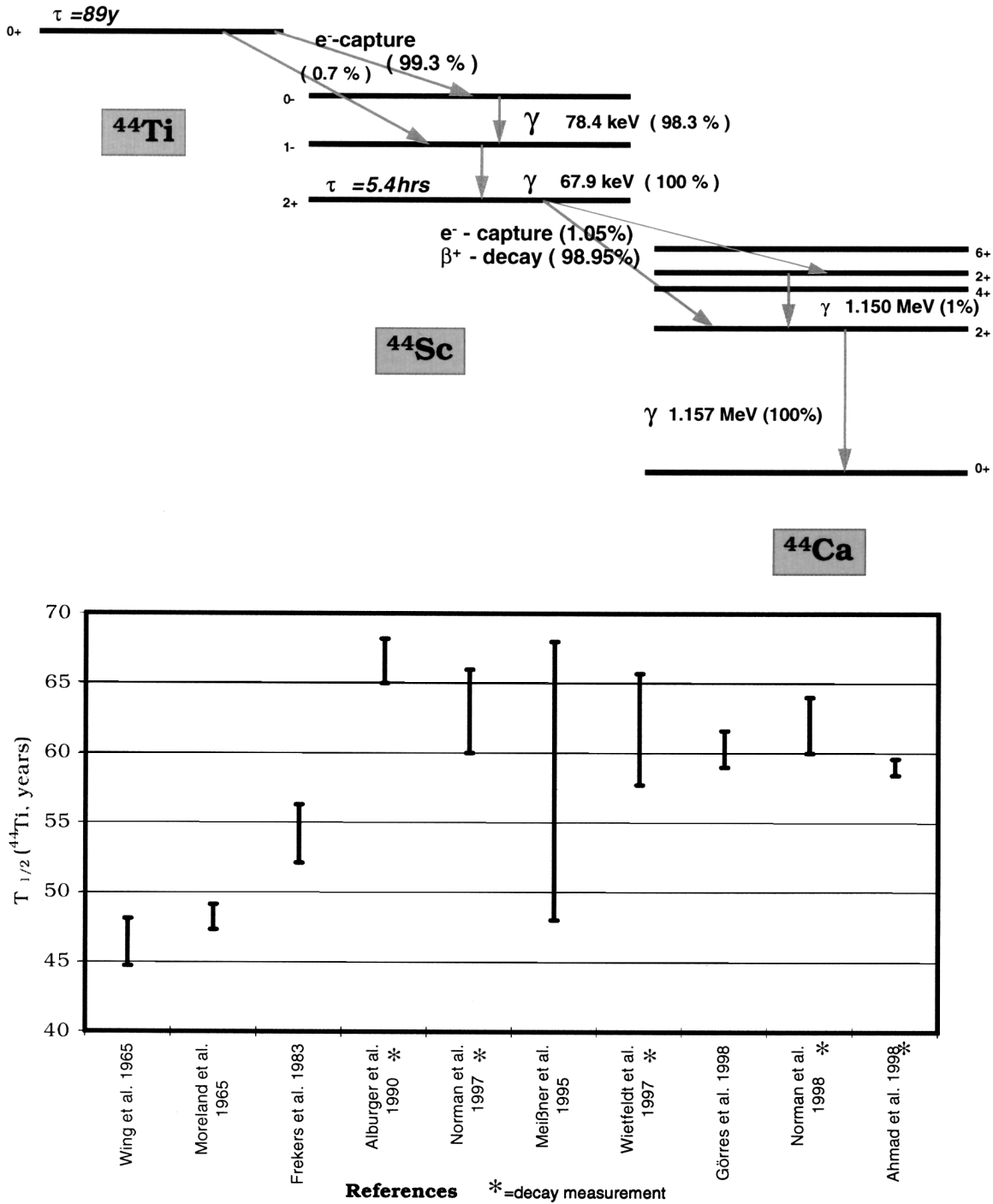


FIG. 6.—Decay of ^{44}Ti (top) and measurements of its half-life (bottom)

beam by the Notre Dame group (Görres et al. 1998) appears convincing, and agrees with two careful new measurements from the decay curve (Ahmad et al. 1998; Norman et al. 1998). This should finally settle this issue, with a half-life of 60 ± 1 yr.

The Cas A supernova remnant is relatively close (2.8–3.7

kpc), young (explosion in A.D. 1668–1680), and wide (physical diameter ~ 4 pc), making it one of the prime sites for studying the composition and early behavior of a supernova remnant. It may only be equaled as SN 1987A unfolds. The discovery of 1157 keV γ -rays from the ~ 300 yr old Cas A supernova remnant (Iyudin et al. 1994; see Fig. 7) was a scientific surprise,

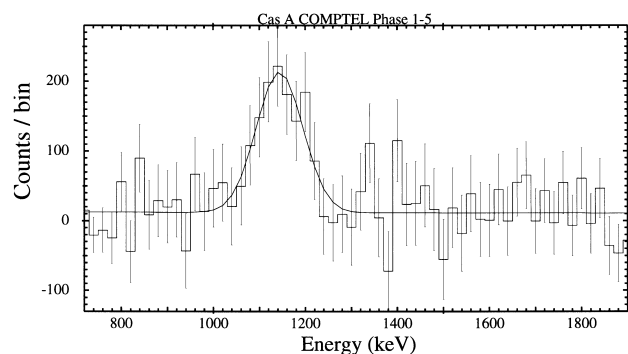


FIG. 7.—Measurement of ^{44}Ti from Cas A (adapted from Iyudin et al. 1997)

because supernova models had indicated $\sim 3 \times 10^{-5} M_{\odot}$ of ^{44}Ti would be ejected (see Fig. 5), which translates into a γ -ray intensity generally below instrument flux sensitivities. Recent analysis of COMPTEL data supports a 5σ detection of Cas A at $4.2 \pm 0.9 \times 10^{-5}$ photons $\text{cm}^{-2} \text{s}^{-1}$ in the 1.157 MeV line (Iyudin et al. 1997), implying $2.4 \times 10^{-4} M_{\odot}$ of ^{44}Ti . Conversion of the measured flux into mass limits must account for the uncertainties in the ^{44}Ti half-life, distance to the event, and the precise time of the explosion.

Data taken with the OSSE instrument, when best-fitted to all three ^{44}Ti γ -ray lines, give an (insignificant) flux value of $1.7 \pm 1.4 \times 10^{-5}$ photons $\text{cm}^{-2} \text{s}^{-1}$ for Cas A (The et al. 1996). The uncertainty of systematic errors in the COMPTEL flux determination, coupled with low OSSE upper limits, confused the community for a while, but the two instruments now appear to yield values that are consistent within their respective uncertainties (Iyudin et al. 1994, 1997; Schönfelder et al. 1996; The et al. 1995, 1996). Measurements of the 68 and 78 keV photons by the *Rossi X-Ray Timing Explorer* result in a marginal flux measurement at $2.87 \pm 1.95 \times 10^{-5}$ photons $\text{cm}^{-2} \text{s}^{-1}$ (Rothschild et al. 1997). Since cosmic-ray interactions in the lead collimator produce fluorescence lines at 74 and 85 keV, along with an iodine activation line present at 66 keV, the detection of ^{44}Ti lines has been more difficult than expected for this experiment. Additional measurements are necessary.

From the γ -ray observations one may constrain the ^{44}Ti half-life by assuming the supernova model yields, a distance to Cas A of 3.4 kpc, and the year of the explosion as ~ 1680 . This procedure also tends to favor the larger ^{44}Ti half-lives, too.

The abundance of ^{44}Ti and ^{56}Ni as a function of mass inside a $25 M_{\odot}$ star is shown in Figure 8 (Timmes et al. 1996a). The mass cut is shown as the solid vertical line. Everything interior to the mass cut becomes part of the neutron star, everything exterior may be ejected, depending on how much mass falls back onto the neutron star during the explosion. Regardless, if ^{44}Ti is ejected, so is ^{56}Ni . The isotope ^{56}Ni is made with ^{44}Ti , in the same mass zone regime, and is 3 orders of magnitude more abundant than ^{44}Ti . A large quantity of ^{56}Ni ejected means a bright supernova. How bright? An abundance of ^{44}Ti as large

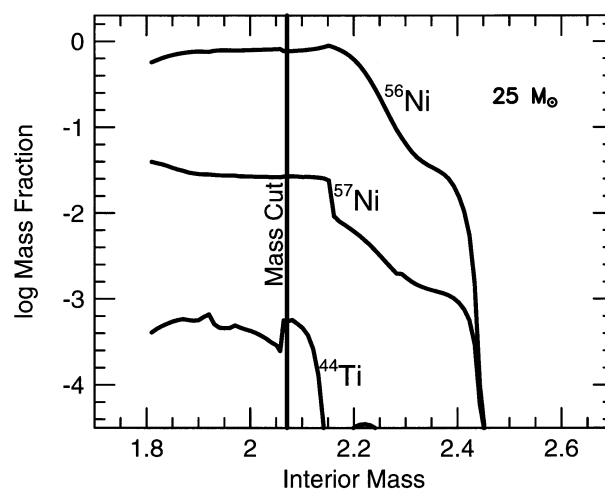


FIG. 8.—Mass profiles of ^{44}Ti and ^{56}Ni for a $25 M_{\odot}$ core-collapse supernova model (adapted from Hoffman et al. 1995).

as reported ($\sim 10^{-4} M_{\odot}$) would probably mean the ejection of at least $0.05 M_{\odot}$ of ^{56}Ni . With or without a hydrogen envelope, the supernova would then have a peak luminosity brighter than the 10^{42} ergs s^{-1} observed for SN 1987A. If no interstellar absorption would attenuate the optical light curve, the Cas A supernova should have had a peak apparent magnitude of -4 , easily recognizable on the sky (Timmes et al. 1996a). Cas A was not widely reported as such; some 10 mag of visual extinction is required to make the γ -ray ^{44}Ti measurements consistent with these historical records (or rather their absence).

There may indeed have been such a large visual extinction to Cas A at the time of the explosion. At a distance of ~ 3 kpc the optical extinction in the plane of the Galaxy has long been estimated to be 4–6 mag. If Cas A was embedded in a dusty region, or experienced significant mass loss that condensed into dust grains before the explosion, the extinction could have been even larger. Measurements of the X-ray scattering halo around Cas A from the *Röntgensatellite* (ROSAT) and the Japanese *Asuka* satellite (ASCA) offer some compelling evidence for a larger reddening correction. ROSAT reports that the scattering halo is unusually low for the derived N_{H} values ($N_{\text{H}} = 1.8 \times 10^{22} \text{ cm}^{-2}$), while this N_{H} is twice as large as an $A_{\text{V}} = 5$ usually implies (Predehl & Schmitt 1995). This can be understood if extra material is distributed close to Cas A, which is relatively dust-free and corresponds to an additional optical extinction of $A_{\text{V}} = 5$ at the time of the supernova—just about what is needed. While hypotheses such as that the explosion took place in a dense molecular cloud or that an optically thick cloud occulted Cas A at the time of the explosion cannot be ruled out, secondary evidence suggest these scenarios are unlikely. A perhaps more natural hypothesis for this local material is the dusty shell of material ejected prior to the explosion as a Type Ib supernova. Measurements of X-ray emission from the remnant by ASCA (see, e.g., Holt et al. 1994) can best be explained by ≈ 6

M_{\odot} of circumstellar material ejected by the presupernova star during its red supergiant phase (Borkowski et al. 1996). The supernova shock wave could have destroyed much of the dust as it propagated through the debris and the material surrounding the Cas A supernova. This scenario explains the lack of optical detection, excess neutral hydrogen column density, dust-free and metal-rich debris, and ejection of $\sim 10^{-4} M_{\odot}$ of ^{44}Ti (Hartmann et al. 1997).

The present nature of the compact remnant in Cas A is ambiguous, with the actual mass at the onset of carbon burning being critical. Deep X-ray imaging around Cas A does not reveal the synchrotron nebula one might expect around a neutron star (Ellison et al. 1994). Deep infrared images taken under excellent seeing conditions have set strict magnitude limits on the presence of a stellar remnant (van den Bergh & Pritchett 1986; Fesen & Becker 1991). Recent *ISO* observations provide a hint toward presupernova dust north of the bright ring of blast-wave-heated dust (Lagage et al. 1996) and supports some local extinction from comparison of infrared to optical images (C. Cesarsky 1997, private communication). The region around the center of Cas A simply appears void of any detectable stars. So observationally, a black hole may have formed. This would make the ejection of a lot of ^{44}Ti more difficult, but not an impossibly rare event. The black hole mass would need to be not too far above the critical gravitational mass of probably less than $2 M_{\odot}$.

Exclusive of any energy input from a pulsar, accreting compact object or circumstellar interaction, SN 1987A is an epoch where the dominant energy source should be from the decay of ^{44}Ti . The thermal luminosity, mostly from e^+ kinetic energy, is expected to be

$$L_{44} = 4.1 \times 10^{36} \left\{ 1 - \exp \left[-\kappa_{44} \phi_0 \left(\frac{t_0}{t} \right)^2 \right] + 1.3 \right\} \\ \times \exp \left(-\frac{t}{\tau_{44}} \right) \left[\frac{M(^{44}\text{Ti})}{1.0 \times 10^{-4}} \right] \text{ ergs s}^{-1},$$

where $\phi_0 = 7.0 \times 10^4 \text{ g cm}^{-2}$ is the column depth at a fiducial time $t_0 = 10^6 \text{ s}$, $\kappa_{44} = 0.04 \text{ cm}^2 \text{ g}^{-1}$ is an estimate of the effective opacity, and τ_{44} is the mean ^{44}Ti lifetime (Woosley, Pinto, & Hartmann 1989). Note that changes in the amount of ^{44}Ti ejected produce a linear shift of the light curve. Bolometric light curves of SN 1987A derived from broadband photometry (Suntzeff et al. 1992; Suntzeff 1998; Bouchet & Danziger 1993) and the above theoretical considerations are shown in Figure 9 for the 500–3500 day period. There are no data points past day 2000, since most of the emission is in the far-infrared wavelength region, where it is not easily observed. Preliminary fits to the latest *UVBRIJHK* light curves show that the cooling time of the remnant is longer than previously thought ($\lesssim 1 \text{ mag}$

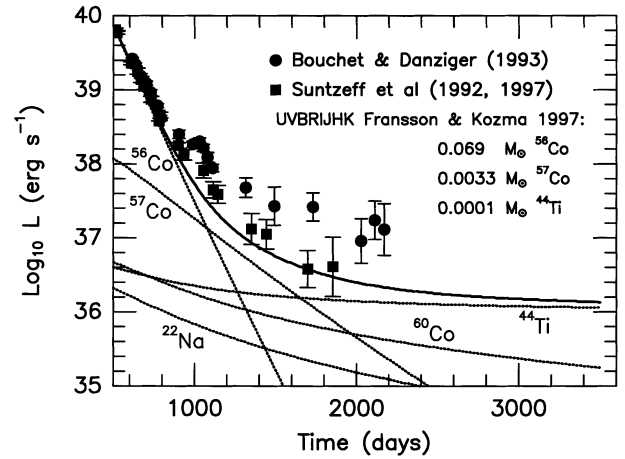


FIG. 9.—Bolometric light curve of SN 1987A

per 1000 days; Suntzeff 1998¹), and suggest $10^{-4} M_{\odot}$ of ^{44}Ti (Fransson & Kozma 1998), the value used in Figure 9 when showing the thermal luminosity deriving from the decay of various radioactive isotopes. The solid line is the total luminosity, assuming that radioactive decay is the sole power source. This energy input may be difficult to resolve uniquely, however, if the atomic processes that convert nuclear decay energy into optical-infrared luminosity are no longer operating in steady state (Clayton et al. 1992; Fransson & Kozma 1993).

Notice that $\sim 10^{-4} M_{\odot}$ of ^{44}Ti is inferred to have been ejected in SN 1987A (a Type II event) and in Cas A (probably a Type Ib event). This agreement may be fortuitous, but it may be evidence for the core-collapse explosion mechanism being well regulated.

For a distance of 50 kpc to SN 1987A and a half-life of 60 yr, $10^{-4} M_{\odot}$ of ^{44}Ti would produce a γ -ray line flux of $2 \times 10^{-6} \text{ photons cm}^{-2} \text{ s}^{-1}$. This line flux is too small for the spectrometers aboard *CGRO*, possibly too small for *INTEGRAL* instruments, but large enough that it might be detected by next-generation γ -ray missions. Spherically symmetric models of SN 1987 A show that the ^{44}Ti that manages to be ejected has a very low speed, typically less than about 1000 km s^{-1} . This would result in very narrow lines. Observations of SN 1987A, especially the broad infrared lines of nickel, early appearance of X-rays, and smoothness of the bolometric light curve, all argue for mixing of ^{56}Ni out to velocities between 2000 and 4000 km s^{-1} (see, e.g., Arnett et al. 1989). The ^{44}Ti may be similarly mixed. It is interesting to know if it is, for it may give us some valuable information about the explosion mechanism and multidimensional mixing.

¹ See also Suntzeff, N. B. 1997, in *Supernovae: Their Causes and Consequences*, ed. A. Burrows, K. Nomoto, & F. Thielemann; www.itp.ucsb.edu/online/supernova/snovaetrans.html.

4.2. ${}^7\text{Be}$ and ${}^{22}\text{Na}$

Classical novae are the most plausible sources for production of possibly detectable 478 keV γ -rays from the decay of radioactive ${}^7\text{Be}$, and the 1.275 MeV γ -ray line from the decay of ${}^{22}\text{Na}$. Other sources such as red giant stars and supernovae also synthesize ${}^7\text{Be}$, but the isotope cannot be transported with sufficient rapidity into regimes that are transparent to γ -rays. The explosion of a massive star also produces ${}^{22}\text{Na}$ in potentially detectable amounts, but classical novae remain a favored candidate due to their relative proximity (known Galactic events) and their relative frequency of occurrence ($\sim 30 \text{ yr}^{-1}$ in the Galaxy). Each of these two isotopes probes different phases of the thermonuclear runaway model. Both have also been a target of γ -ray astronomy for quite some time (Hoyle & Clayton 1974).

Nuclei of mass $A = 7$ are formed predominantly through the ${}^3\text{He}(\alpha, \gamma){}^7\text{Be}$ reaction (Fig. 10), whether in classical nova explosions, hydrostatic red giant envelopes, or primordial nucleosynthesis scenarios. In novae, the ${}^3\text{He}$ seed material originates mainly from the accreted material and to a much lesser extent from incomplete hydrogen burning (first two steps of the hydrogen-burning proton-proton chain). Competing with the ${}^3\text{He}(\alpha, \gamma)$ reaction in the consumption of ${}^3\text{He}$ is ${}^3\text{He}({}^3\text{He}, 2p){}^4\text{He}$ reaction. This third step of the proton-proton chain is always faster, except at very low ${}^3\text{He}$ abundances. Accordingly, the final ${}^7\text{Be}$ yields from novae display a logarithmic, not a linear, dependence on the initial ${}^3\text{He}$ content (Boffin et al. 1993). A solar ${}^3\text{He}$ mass fraction in the accreted envelope cannot generate a ${}^7\text{Li}$ (${}^7\text{Be}$) abundance that greatly exceeds the solar mass fraction.

After ${}^7\text{Be}$ is produced, it is destroyed mainly by proton captures to form ${}^8\text{B}$. This destruction is quite efficient below temperatures of $\sim 10^8 \text{ K}$ and densities above $\sim 100 \text{ g cm}^{-3}$. At hotter temperatures the photodisintegration of ${}^8\text{B}$ reduces the overall destruction somewhat. Including the leakage of ${}^8\text{B}$ to ${}^9\text{C}$ is important, since it reduces the ${}^7\text{Be}$ abundances by allowing a flow out of any ${}^7\text{Be}$ - ${}^8\text{B}$ equilibrium (Boffin et al. 1993). Once the nuclear reactions cease, any remaining ${}^7\text{Be}$ will β -decay to ${}^7\text{Li}$ with a half-life of 76 days, and produce the 487 keV photon that is a target of γ -ray astronomy. Assuming a nova ejects a total mass of $10^{-4} M_{\odot}$, of which the ${}^7\text{Be}$ mass fraction is 5×10^{-6} , the 487 keV flux is shown as a function of time in Figure 10 for a distance to the nova of 0.5 kpc. These values may not be typical, and preferences for other values are easily accommodated; the flux scales linearly with the total ejected mass and ${}^7\text{Be}$ mass fraction while scaling with the inverse square of the distance. For the conditions shown, a space-borne spectrometer with a sensitivity of 10^{-5} photons $\text{cm}^{-2} \text{ s}^{-1}$ will be able to study such novae for about 3 months.

Convective processing and mixing timescales in nova envelopes are critical issues. Significant γ -ray signals from ${}^7\text{Li}$ can only occur when convection can transport freshly synthesized ${}^7\text{Be}$ into a cooler and less dense region. Spherically sym-

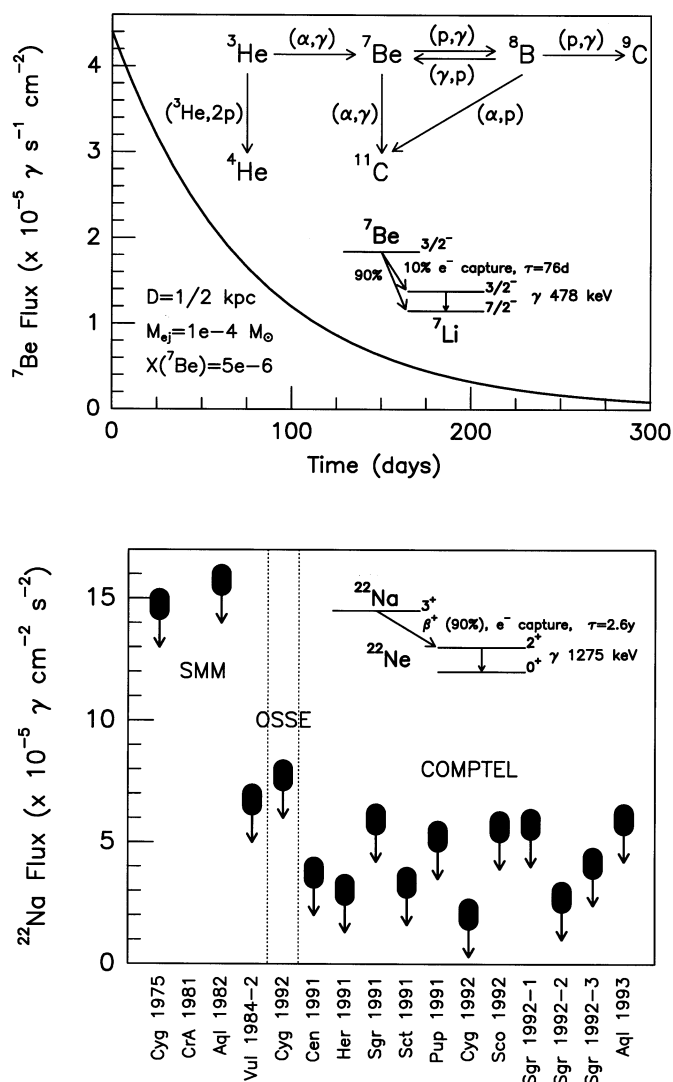


FIG. 10.— ${}^7\text{Be}$ decay scheme and production processes (top) and ${}^{22}\text{Na}$ measurements from individual novae (bottom).

metric models of classical novae that incorporate time-dependent convection and the accretion phase tend to give ${}^7\text{Be}$ yields between 10^{-12} and $10^{-10} M_{\odot}$ depending on the mass and composition of the white dwarf and accreted material (Politano et al. 1995). Two-dimensional hydrodynamic models that examine the evolution of a fully convective hydrogen-rich envelope during the earliest stages of the thermonuclear runaway are beginning to be calculated and should help clarify some of these uncertainties in the future (Shankar & Arnett 1994; Glasner, Livne, & Truran 1997).

The effect of the white dwarf mass and composition also plays a crucial role in the resulting nucleosynthesis. Less massive white dwarfs generally support a larger accreted envelope mass before ignition occurs. More massive envelopes ignite material at the core-envelope interface at a larger density (de-

generacy) and achieve a higher peak temperature. This results in stronger outbursts with shorter evolutionary timescales and extends the nuclear activity toward higher Z nuclei (José & Hernanz 1998). While isotope production is thus generally enhanced when the initial mass of the underlying white dwarf is increased, less material is accreted before the fuel ignites in more massive white dwarfs, and the total mass of matter lifted out of the gravitational well is smaller. In addition, the less ^{12}C that is present during the runaway, the less nuclear energy is released by the CNO cycle at a given temperature, and the less light isotope production there is. Estimates for mass of ^7Li ejected in the carbon-oxygen white dwarf models are almost an order of magnitude larger than the corresponding (same core mass) oxygen-neon white dwarf models. It should also be emphasized that the mass accretion rate and the initial white dwarf luminosity (or temperature) may also influence the results. More violent outbursts are obtained when lower mass accretion rates or lower initial luminosities are adopted, since a higher level of degeneracy is attained (José & Hernanz 1998). The expected effect on the resulting nucleosynthesis is an extension of the nuclear activity toward heavier species as the mass accretion rate or the initial luminosity decreases because of the higher temperatures achieved in the envelope.

There have been no reported detections of 478 keV line emission from either the cumulative effects of many novae (~ 100) near the Galactic center region, or individual novae. However, *SMM* reported a 3σ upper limit flux of 1.7×10^{-4} photons $\text{cm}^{-2} \text{s}^{-1}$, assuming a point source of constant intensity at the Galactic center (Harris, Leising, & Share 1991). They also reported 3σ upper limit fluxes of 2.0×10^{-3} photons $\text{cm}^{-2} \text{s}^{-1}$ from Nova Aql 1982, 8.1×10^{-4} photons $\text{cm}^{-2} \text{s}^{-1}$ from Nova Vul 1984, and 1.1×10^{-3} photons $\text{cm}^{-2} \text{s}^{-1}$ from Nova Cen 1986. These results imply upper limit ^7Be abundances that are about an order of magnitude above even the most optimistic theoretical expectations, and thus are not very constraining.

The radioactive isotope ^{22}Na is synthesized in classical novae at the interface between the white dwarf and the accreted envelope. How much carbon, oxygen, magnesium, and neon is dredged up from the white dwarf or accreted from the binary companion is a critical issue for determining the strength of any ^{22}Na γ -ray signal. The chief nuclear flows that create and destroy ^{22}Na are discussed in detail by Higdon & Fowler (1987) and Coc et al. (1995), along with the uncertainties in several key reaction rates. As the ejecta cools and expands, and nuclear burning ceases (~ 7 days), ^{22}Na decays with a half-life of 2.6 yr from the $J^\pi = 3^+$ state to a short-lived excited state of ^{22}Ne , emitting a 1.275 MeV γ -ray line in the process (Fig. 10).

Gamma-ray line emission at 1.275 MeV from classical novae in the Milky Way remains to be positively detected. *SMM*, *OSSE*, and *COMPTEL* have, however, reported upper limits for several individual novae (Leising 1993; Iyudin et al. 1995; see Fig. 10). The 2σ upper limit fluxes reported by *COMPTEL* put tight constraints on thermonuclear runaway models of clas-

sical novae. The category “neon nova” has been suggested for nova events that display strong neon features (i.e., show large metal enrichments) at optical wavelengths (Starrfield et al. 1996). For neon-novae, which are expected to eject the largest ^{22}Na masses, the average *COMPTEL* upper limit flux of 3×10^{-5} photons $\text{cm}^{-2} \text{s}^{-1}$ translates into an upper limit on the ejected ^{22}Na mass of $3.7 \times 10^{-8} M_\odot$ (Iyudin et al. 1995).

Spherically symmetric models of classical novae that incorporate a more self-consistent treatment of the hydrodynamic evolution and refined initial white dwarf compositions tend to give ^{22}Na yields of $\sim 10^{-8} M_\odot$ for the most favorable neon-novae cases (Starrfield et al. 1996). In general, these recent improvements to the modeling have reduced the ^{22}Na yield by about an order of magnitude compared to the older models (Weiss & Truran 1990; Starrfield et al. 1992, 1993), which lacked these refinements and were at distinct odds with the *COMPTEL* measurements. It may still be that present nova models are biased from the observations of a few exceptional events and that the typical neon-novae ejects much less mass into the interstellar medium than the exceptional events.

4.3. ^{56}Ni and ^{57}Ni

A goal of observational γ -ray astronomy for the last three decades has been detection of line radiation from the decay of radioactive ^{56}Ni and ^{56}Co produced in supernovae (Clayton, Colgate, & Fishman 1969; see Fig. 11). Type Ia events are favored over the other supernova classes because they produce an order of magnitude more ^{56}Ni than the other types ($\sim 0.6 M_\odot$; Thielemann, Nomoto, & Yokoi 1986) and because they expand rapidly enough to allow the γ -rays to escape before all the fresh radioactivity has decayed. Even so, detection of these events has been difficult to achieve.

Type Ib supernovae synthesize 5–10 times less ^{56}Ni than a typical Type Ia, but expand almost as rapidly as Type Ia supernovae. Thus, their signal is intermediate between Type II and Type Ia. The γ -ray line detection of any Type II supernova outside the Local Group is very improbable. The best-studied supernova of all in radioactive line emission was the Type II supernova SN 1987A (e.g., Arnett et al. 1989), mainly because of its proximity. Detection of ^{56}Co and ^{57}Co lines from SN 1987A by many experiments gave the first extragalactic γ -ray line signal from radioactive isotopes. The early appearance of ^{56}Co γ -radiation presented evidence for enhanced mixing of supernova products within the envelope.

Later, *OSSE* reported detection of ^{57}Co radiation from SN 1987A, with a measured flux of $\sim 10^{-4}$ photons $\text{cm}^{-2} \text{s}^{-1}$ between 50 and 136 keV (Kurfess et al. 1992). For models with low ^{57}Co optical depths, the observed γ -ray flux suggested that the $^{57}\text{Ni}/^{56}\text{Ni}$ ratio produced by explosion was about 1.5–2.0 times the solar system ratio of $^{57}\text{Fe}/^{56}\text{Fe}$ (Clayton et al. 1992; see Fig. 9). Estimates of SN 1987A’s bolometric luminosity at optical and infrared wavelengths at day 1500, while indicating that ^{57}Co was indeed powering the light curve at that time,

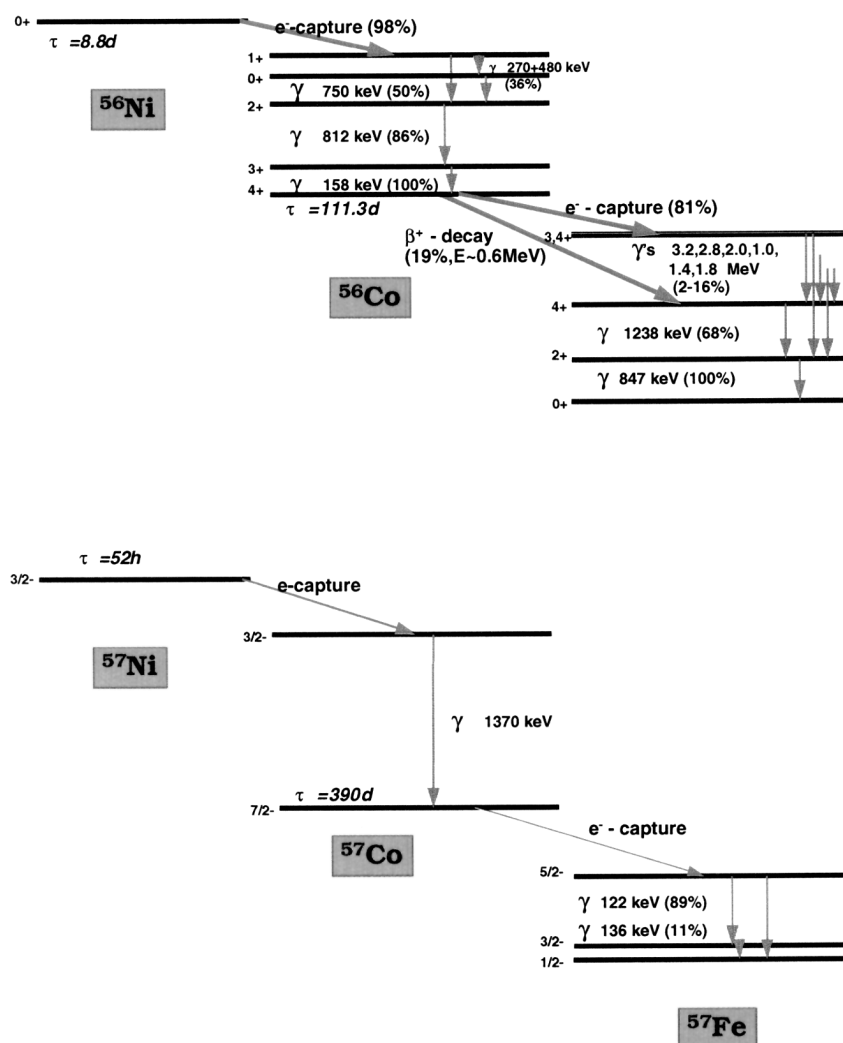


FIG. 11.—Decay of ^{56}Ni to ^{56}Fe and ^{57}Ni to ^{57}Fe , illustrating the most significant spin-parity levels and γ -ray photons. The most important transitions for γ -ray line astronomy and supernova diagnostics are marked with an asterisk.

seemed to indicate a $^{57}\text{Ni}/^{56}\text{Ni}$ ratio that was 5 times the solar $^{57}\text{Fe}/^{56}\text{Fe}$ ratio (Suntzeff et al. 1992; Dwek et al. 1992). However, preliminary fits to the latest *UVBRIJHK* light curves show that the cooling time of the remnant is longer than previously thought ($\lesssim 1$ mag per 1000 days; Suntzeff 1998), reducing the demand for heating from radioactive ^{57}Co . These preliminary fits give $0.069 M_{\odot}$ of ^{56}Co and $0.0033 M_{\odot}$ of ^{57}Co (Fransson & Kozma 1993, 1998; see Fig. 9). This gives a $^{57}\text{Ni}/^{56}\text{Ni}$ ratio of twice the solar $^{57}\text{Fe}/^{56}\text{Fe}$ ratio and is in reasonable agreement with the ratio implied by the OSSE measurements.

Only one Type Ia supernova has been seen in γ -rays, SN 1991T in NGC 4527 (Morris et al. 1995, 1998; see Fig. 12). This galaxy is ~ 17 Mpc distant (determined from Cepheids) and in the direction of the Virgo Cluster. The supernova was unusually bright at maximum ($0.7 M_{\odot}$ of ^{56}Ni ; Höflich et al.

1996), and the light curve evolved unusually slowly. The classification as a peculiar Type Ia event is based on the absence of the silicon lines so typical in early Type Ia spectra. In addition, the Fe III lines were unusually strong at early epochs. Since no other iron group lines were observed at this time, this iron was probably not a fresh nucleosynthetic product. The spectra did become more typical of Type Ia events at later epochs when the expanding debris became more transparent. Detection of high-velocity ($\sim 13,000\text{ km s}^{-1}$) iron and nickel in the outer layers of SN 1991T favors models in which the subsonic flame front propagates larger distances from the white dwarf core before making the transition to a detonation. These types of delayed-detonation models are also consistent with the velocity profile of most of the other ejecta (silicon, calcium) seen in SN 1991T. Shigeyama et al. (1993) suggest that detection in the early light curve of the 812 keV γ -ray line from

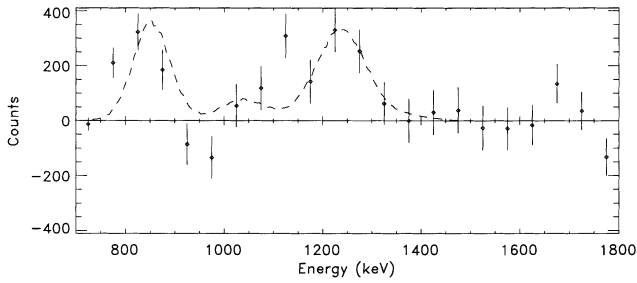


FIG. 12.—SN 1991T spectrum as measured by COMPTEL, after subtraction of a background model (adapted from Morris et al. 1995, 1998).

the decay of ^{56}Ni (Fig. 11) would be direct evidence for delayed-detonation models, since the line cannot be seen when the ^{56}Ni is embedded deeper in other categories of Type Ia models. However, sub-Chandrasekhar mass models of Type Ia supernova, especially those of white dwarfs in a binary system, are discussed as well. These models may be favorable for ejecting a larger than average ^{56}Ni mass and seek to explain some of the other early light-curve peculiarities as arising from interactions of the supernova debris with the thick disk of material that surrounded the merger.

The tentative COMPTEL detection of the ^{56}Co decay γ -rays indicates that this isotope was present in the outer envelope, and thus supports extensive mixing scenarios. The COMPTEL measurement converts into a surprisingly large ^{56}Ni mass, however, between $1.3 M_{\odot}$ (for a distance of 13 Mpc; Morris et al. 1995) and $2.3 M_{\odot}$ for the 17 Mpc favored currently (P. Ruiz-Lapuente 1997, private communication). This requires that almost all of the Chandrasekhar mass white dwarf must be turned into radioactive ^{56}Ni . The OSSE upper limits (Leising et al. 1995) may indicate that the ^{56}Co line flux derived by Morris et al. (1995) is too high, although the detection itself is confirmed at the same 3–4 σ significance (Morris et al. 1998). More detections of Type Ia supernovae in ^{56}Ni are required to clarify how typical SN 1991T was. COMPTEL and OSSE will hopefully remain ready to observe any nearby events (for estimates see below).

5. ASSOCIATED ASTROPHYSICAL CHALLENGES

5.1. Meteoritic Grains

Although the nucleosynthetic processes occurring in different stars generally result in a wide range of isotopic compositions, by far most of the material from the many stellar sources that contributed to the protosolar cloud was thoroughly processed and mixed, which resulted in the essentially isotopically homogeneous solar system we know today. A small fraction of the original material, in the form of presolar dust grains, survived solar system formation and became trapped in primitive meteorites. From their highly unusual isotopic compositions, relative to that of the solar system, these presolar grains

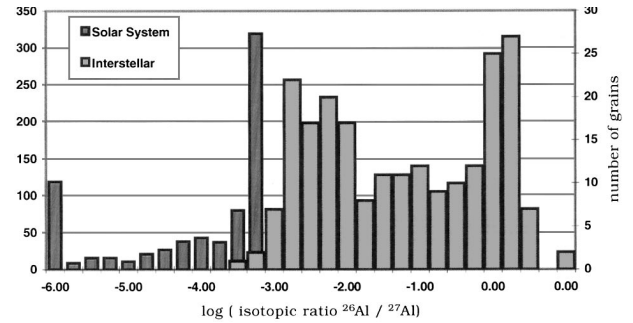


FIG. 13.—Histogram of inferred $^{26}\text{Al}/^{27}\text{Al}$ for interstellar grains of various types (*wide hatched columns*) and solar system objects (*narrow filled columns*), adapted from MacPherson et al. (1995).

are inferred to have formed in circumstellar atmospheres or, in some cases, in nova or supernova explosions. Because their compositions reflect the isotopic and chemical signatures of their sources, presolar grains provide direct information about stellar evolution and nucleosynthesis, mixing processes in stars, the physical and chemical conditions of stellar atmospheres, and the chemical evolution of the Galaxy (Anders & Zinner 1993; Ott 1993).

There are several interesting parallels between ^{26}Al , ^{22}Na , ^{44}Ti , and ^{60}Fe in γ -ray astronomy and in the laboratory study of presolar meteoritic grains. Enhanced $^{26}\text{Mg}/^{24}\text{Mg}$ ratios in the calcium-aluminum (Ca-Al) rich inclusions of the Allende meteorite were the first evidence for live ^{26}Al in the early solar system (Lee, Papanastassiou, & Wasserburg 1977). Present compilations (MacPherson et al. 1995), with over 1500 data points derived from various types of meteoritic samples, confirm the enhancements in ^{26}Mg in these old and stable inclusions of solar system material and show a homogeneous isotopic ratio $^{26}\text{Al}/^{27}\text{Al}$ of $\sim 5 \times 10^{-5}$. This is interpreted as the in situ decay of ^{26}Al in the early protosolar droplets (MacPherson et al. 1995), mainly from the strong correlation of ^{26}Mg excess with aluminum abundances of the samples. This is direct evidence of an injection of (at least) ^{26}Al into the solar nebula shortly before solar system formation. The inferred $^{26}\text{Al}/^{27}\text{Al}$ ratio of $\sim 5 \times 10^{-5}$ is substantially larger than the ratio of $2\text{--}3 \times 10^{-6}$ estimated from γ -ray measurements (Diehl et al. 1995).

Figure 13 compares the inferred initial $^{26}\text{Al}/^{27}\text{Al}$ ratio distributions of presolar grains (corundum, graphite, and silicon carbide) with the total population of data for aluminum-rich material (mostly Ca-Al rich inclusions) that represents solar system aluminum. There is very little overlap between the two populations. This ensures that these types of meteoritic samples constitute different observational windows that need not correlate. Rather, each distribution carries imprints of the specific grain formation or even early solar system processes (see MacPherson et al. 1995).

An indication that live ^{60}Fe also existed when the meteorites solidified is found from isotopic analysis of the Chernovny Kut meteorite (Shukolyukov & Lugmair 1993). The measured excess of ^{60}Ni , after alternative modes of production such as spallation and (n, γ) reactions on ^{59}Co could be eliminated, leads to a $^{60}\text{Fe}/^{56}\text{Fe}$ ratio at the time of iron-nickel fractionation of $\sim 7.5 \times 10^{-9}$. This is consistent with the inferred 10 million year hiatus before the formation of the Ca-Al rich inclusions in the Allende meteorite, which has a much larger $^{60}\text{Fe}/^{56}\text{Fe}$ ratio at the time of fractionation of $\sim 1.6 \times 10^{-6}$ (Birck & Lugmair 1988). However, the possibility that some of the ^{60}Ni in the Ca-Al rich inclusions is fossil rather than from the in situ decay of ^{60}Fe cannot be excluded.

Despite their rarity, noble gases have played a key role in establishing the interstellar origin of diamond, graphite, and silicon carbide. Neon has three stable isotopes, permitting complex mixtures to be resolved into their components. One of the components, Ne-E, exists in two varieties that differ in both thermal release temperature of the neon and the density of the carrier, and hence are designated “H” (high) and “L” (low). High-precision measurements show that Ne-E(H) is not radiogenic ^{22}Ne from the decay of ^{22}Na , but primary neon. The strongest evidence for a parentless origin of Ne-E(H) comes from direct measurement of ~ 160 individual silicon carbide grains by laser gas extraction. In each case, the ^{22}Ne is accompanied by an amount of ^4He that is a close match with the expected helium-shell composition of stars with a mass $\lesssim 3 M_{\odot}$ and Fe/H near solar (Nichols et al. 1993; Lewis, Amari, & Anders 1993). No such helium accompanies Ne-E(L) from graphite spherules, and so for Ne-E(L), a major contribution from radioactive ^{22}Na is a viable, even preferred explanation (Gallino et al. 1990; Brown & Clayton 1992; Zinner 1997).

Large excesses in ^{44}Ca have been observed in four low-density graphite grains and five silicon carbide grains of Type X extracted from the Murchison meteorite and have been shown to be related to the radioactive decay of ^{44}Ti (Nittler et al. 1996; Hoppe et al. 1996; see Fig. 6). Because ^{44}Ti is produced only in supernovae, these grains must have a supernova origin. Moreover, the silicon, carbon, nitrogen, aluminum, oxygen, and titanium isotopic compositions of these large grains ($>1 \mu\text{m}$) reflect the isotopic composition expected from a Type II supernova source (Nittler et al. 1996). This is also strong evidence that these grains are supernova condensates and provides evidence for deep and heterogeneous mixing of different supernova regions, including the nickel core.

Extensive high-precision measurements of other meteorites have found many other anomalous abundance ratios, and these are generally attributed to isotopes that were still radioactive during the decoupling of the solar nebula from the interstellar medium 4.6 Gyr ago (see, e.g., Harper 1996). These measurements have led to hypotheses of the solar system formation being related to a nearby event such as a supernova or an AGB star (Cameron 1993; Wasserburg et al. 1995). In other words,

the solar nebula experienced an enrichment in relatively short-lived radioactive isotopes. Whether this enrichment is caused by the hypothesized triggering events (if they occurred) or some unconsidered process during formation of the Sun remains an active area of research.

Shu et al. (1997) discuss the idea that the chondrules and Ca-Al rich inclusions found in chondritic meteorites might have been formed as solids entrained and melted in the bipolar wind that results from the interaction of the accreting protosolar nebula and the magnetosphere of the young proto-Sun. Aerodynamic sorting and a mechanical selection for molten droplets that rain back onto the disk at planetary distances explain the size distributions and patterns of element segregation that we observe in carbonaceous and ordinary chondrites. Cosmic-ray ions generated in the flares that accompany the general magnetic activity of the inner region may irradiate the precursor rocks before they are launched in the bipolar wind. Under certain scaling assumptions for the efficiency of the process in protostars, Shu et al. find that cosmic-ray bombardment can generate the short-lived radionuclides ^{26}Al , ^{41}Ca , and ^{53}Mn at their inferred meteoritic levels. Simply put, this mechanism captures material trying to get on the Sun, heats it up, irradiates it with cosmic rays, and dumps it back onto the disk farther out (Glanz 1997). It is far from clear, however, that such low-energy cosmic rays can explain most of the complex isotopic patterns found in chondrites. Additional measurements are necessary to see if the isotopic anomalies are best explained by such a single mechanism.

5.2. Positrons from Radioactivities

Radioactive decays can generate positrons whenever the energy level of the daughter atom is below the energy level of the parent by more than the 1.022 MeV pair production threshold. Interesting numbers of positrons are produced from the β^+ -decay of ^{26}Al , ^{44}Ti , ^{56}Co and the distinct nova products ^{13}N and ^{18}F . Annihilation produces two 511 keV photons if the positron and electron spins point in opposite directions, or three photons in a continuous energy spectrum if the spins are parallel. The three-photon annihilation process usually involves formation of positronium, which then decays before being collisionally destroyed because of the low densities of interstellar space. As a result, the fraction of positronium radiation in the total annihilation signal carries information about the thermodynamic properties of the annihilation environment. A cold, neutral environment results in positronium fractions of 0.9–0.945 (Bussard, Ramaty, & Drachman 1979; Brown, Leventhal, & Mills 1986), while larger positronium fractions tend to indicate annihilation in warmer environments, 5×10^3 K or hotter. The positrons produced by the interesting radioactive decays have average kinetic energies of $\sim \text{MeV}$, and thus are relativistic. Deceleration and thermalization are more likely than annihilation in flight, so that the positron lifetime in in-

terstellar space before annihilation is $\sim 10^5$ yr (Lingenfelter, Chan, & Ramaty 1993; Ramaty & Lingenfelter 1995). This thermalization process means intrinsically narrow 511 keV line widths that are related to the annihilation environment rather than to the positron production environment.

In addition to annihilation from radioactive decays, positron annihilation is expected from the disks around accreting compact remnants, from the jets caused by dynamo action of accreting compact sources, and from γ - γ reactions in strong magnetic fields. How can these various signals be differentiated? Positrons from radioactive decays usually annihilate in the diffuse interstellar medium where the thermalization lifetime is long. Positrons produced around compact objects should annihilate near the compact objects, since the density is usually much larger in those environments. This is expected to result in a more localized and possibly time-variable signal. Such annihilation spectra may also contain such recognizable signatures as a high-energy tail above 511 keV from annihilation in flight, a blueshift from positron jets moving toward the observer, a redshift when originating from sources with a large gravitational field, or a distinctly smaller positronium fraction.

Observations of the 511 keV line from positron annihilation show a steady diffuse component from the Galactic disk superimposed upon a time-variable point source located near the Galactic center (Johnson, Harden, & Haymes 1972; Ramaty, Skibo, & Lingenfelter 1994). OSSE measurements of the annihilation radiation can be analyzed in terms of plausible spatial distribution models that aim to separate the disk component from the Galactic bulge component (Kinzer et al. 1996; Smith, Purcell, & Leventhal 1998). This decomposition finds annihilation rates of $10^{43} e^+ s^{-1}$ for the disk and $2.6 \times 10^{43} e^+ s^{-1}$ for the bulge. Almost all of the annihilation luminosity from the Galactic disk may be explained by radioactive sources. About $16\% \pm 5\%$ is assigned to ^{26}Al , with the remainder partitioned between ^{44}Ti , ^{56}Co , and old stellar population products (Timmes et al. 1996a; Lingenfelter et al. 1993). Kinzer et al. (1996) determined a positronium fraction of 0.94–1.0 for the inner Galaxy, suggesting that the contribution from compact sources might be small. However, this constraint strongly depends on the environment of the compact sources; Ramaty et al. (1994) point out that the entire bulge component could be explained from 1E 1740.7–2942 alone if positrons are not rapidly annihilated in a target close to that compact source. Hernanz et al. (1996) estimate from their simulations of classical novae that the peak 511 keV emission reaches $\sim 10^{-2} (D/1 \text{ kpc})^2$ photons $\text{cm}^{-2} \text{ s}^{-1}$ for a period of about 7 hr after the outburst. This would make detections from distances as far as the Galactic center feasible, if timing with the observations were fortunate. Overall, however, the nova contribution to the diffuse 511 keV glow of the Galaxy is expected to be low (Lingenfelter & Ramaty 1989; Ramaty & Lingenfelter 1995).

5.3. Galactic Nucleosynthesis and Supernova Rates

Direct measurement of the Milky Way's supernova rate is notoriously difficult. Various methods have been attempted, such as O–B2 star counts within 1 kpc of the Sun, radio supernova remnant counts, γ -ray fluxes from the decay of ^{44}Ti , neutrino burst detections, and pulsar birthrate estimates. These indirect methods incur large errors and only yield upper limits for cases based on incomplete observations. Galactic supernova rates have therefore been based on extragalactic supernova searches. These estimates depend upon morphological type, Hubble constant, completeness of the surveys, determination of reliable control times, and the uncertain luminosity of the Galaxy. The total blue luminosity, $H\alpha$, and far-infrared fluxes of the Milky Way remain uncertain, in contrast to those of most Local Group galaxies. Nevertheless, using the extragalactic estimates with a total Galactic blue luminosity of $2.3 \times 10^{10} L_{\odot}$, a Hubble constant of $75 \text{ km s}^{-1} \text{ Mpc}^{-1}$, and a Sbc Galactic morphology, the Galactic core-collapse supernova rate is estimated to be 2.4–2.7 per century, while the Type Ia rate is estimated to be 0.3–0.6 per century (van den Bergh & McClure 1994; Tammann, Löffler, & Schröder 1994). Thus, the total supernova rate is about 3 per century and the ratio of core collapse to thermonuclear events is about 6.

There are six known local supernovae: Lupus (SN 1006) is considered to have been a Type Ia event, Cas A (SN 1680) and Tycho (SN 1572) were most likely Type Ib supernovae, and the Crab (SN 1054), SN 1181, and Kepler (SN 1604) were probably Type II events. This listing may be complete to ~ 4 kpc. For an exponential disk with a 4 kpc scale length extending between 3 and 15 kpc, about 9% of all Galactic OB stars will be located within 4 kpc of the Sun. At a radial distance of 8.5 kpc, the number of supernovae with massive progenitors within 4 kpc of the Sun may be estimated as $\sim 0.09 \times 0.85 \times 3 \sim 2.3$ per millennium (van den Bergh & McClure 1994). This is close to the observed number that are known to have occurred within 4 kpc of the Sun during the last 2000 years. However, the statistical uncertainty in the frequency with which supernovae of different types occur in galaxies of different Hubble class is large, and this agreement may be fortuitous.

The total ^{44}Ti line flux originating from the central regions of the Milky Way was sought by the large field-of-view spectrometers aboard the *HEAO 3* and *SMM* satellites. Analysis of the data taken with *HEAO 3* gave an upper limit of 2×10^{-4} photons $\text{cm}^{-2} \text{ s}^{-1}$ on the Galactic 67.9 and 78.4 keV emission (Mahoney et al. 1992). Searching through nearly 10 years of data taken by *SMM* gave an upper limit of 8×10^{-5} photons $\text{cm}^{-2} \text{ s}^{-1}$ for the inner 150° of the Milky Way in the 1.157 MeV line (Leising & Share 1994); the imaging COMPTEL instrument sets upper limits below 2×10^{-5} photons $\text{cm}^{-2} \text{ s}^{-1}$ for the known historical events (Dupraz et al. 1997).

A first COMPTEL 1.07–1.25 MeV background-subtracted

sky map is shown in Figure 14 (Dupraz et al. 1997). Even though only part of the data has been used in this analysis and the potentially more sensitive background modeling from adjacent energies has not been employed, first conclusions can be drawn: Cas A is the only historic event detected (at $\sim 5 \sigma$ now; see discussion above). Upper limits to the ^{44}Ti line flux from Tycho and Kepler are about half the Cas A signal. Even with the longest ^{44}Ti half-lives measured, Lupus, Crab, and SN 1181 are far too old to have significant amounts of ^{44}Ti remaining to be detected. No previously unknown event is found, even though COMPTEL's sensitivity should provide complete sampling of the last century beyond the distance of the Galactic center.

Core-collapse supernovae and Chandrasekhar mass thermonuclear supernovae tend to account for about one-third of the solar ^{44}Ca abundance, with most of the production attributable to Type II events. The mass of ^{44}Ca produced as itself is comparable to the ^{44}Ca synthesized from the radioactive decay of ^{44}Ti . Even at this $\sim \frac{1}{3}$ solar level, the sky should contain several mean Type II supernova remnants bright enough to be seen in their ^{44}Ti afterglow. However, no search (*HEAO 3*, *SMM*, *COMPTEL*, *OSSE*) has produced a detection of ^{44}Ti line emission from any young, previously unknown, and visually obscured remnants. We simply do not see the expected number of supernova remnants emitting γ -rays from the decay of radioactive ^{44}Ti . After eliminating alternative modes of increasing the ^{44}Ca production (e.g., larger yields), the conclusion becomes almost inescapable. The solar abundance of ^{44}Ca is apparently due to rare events with exceptionally high ^{44}Ti yields. This conclusion was already derived from the *SMM* upper limits to ^{44}Ti γ -rays (Leising & Share 1994). Rare events could mean Type II events where the explosion energy is large enough to minimize the mass of ^{44}Ti that falls back onto the compact remnant, or Type Ia events that manage to explode a sub-Chandrasekhar mass white dwarf. Mapping the Galaxy in ^{44}Ti should help to resolve the unknown rate of these rare events; they would still mark bright spots in the 1157 keV sky. The COMPTEL survey will provide the ultimate database; the result from the first three mission years (Dupraz et al. 1997) still appears inconclusive in this respect.

Integrated nucleosynthesis measurements, such as the 1.809 MeV ^{26}Al observations, can be a useful measure of the Galactic supernova rates. If a dominating origin of ^{26}Al from massive stars is adopted (Prantzos & Diehl 1996), then the γ -ray data combined with nucleosynthesis yields provide independent measures of the massive star formation rate in the Galaxy. The core-collapse supernova rate determined in this way appears consistent with various classical rate determination methods, such as on $\text{H}\alpha$ measurements and supernova records in "similar" distant galaxies (Timmes et al. 1997). Crucial to such an analysis is the integrated radioactive mass inferred from the γ -ray measurements and attributed to massive stars and the spatial distribution of the emission in the Galaxy. But given the wide

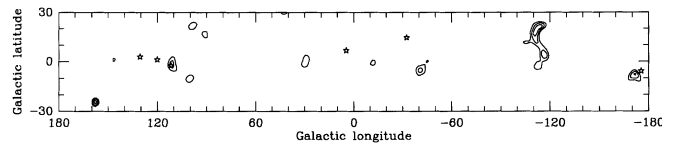


FIG. 14.—A first COMPTEL map of the Galactic plane in the 1.157 MeV line from ^{44}Ti (adapted from Dupraz et al. 1997), using the first 3 yr of data. Star symbols mark locations of historical supernova 1181, Tycho, Cas A, Kepler, Lupus, and Crab (from left to right). The Cas A signal in these data corresponds to 3.5σ significance; likelihood contour levels are in 1σ steps for known sources, $\sim 0.75 \sigma$ for search of new sources.

range of $0.4\text{--}3.5 M_{\odot}$ from present data, γ -ray measurements cannot help resolve the various systematic uncertainties present in the classical methods (e.g., galaxy type, Hubble constant, sample completeness). Future measurements of the position and shape of the 1.809 MeV γ -ray line may provide the basis for a three-dimensional deconvolution of the apparent emission (Gehrels & Chen 1996). Note that the measurement of a 6 keV wide 1.809 MeV line by GRIS (Naya et al. 1996) suggests that any 0.1–0.9 keV line shifts expected from Galactic rotation may be drowned in (yet to be found) broadening processes and hence not allow a direct mapping of the emission.

5.4. Other Galaxies

In undertaking searches for γ -ray line signals from extragalactic supernovae, it is useful to have some guidelines as to what might be expected. With recent catalogs of supernova events, and distances based upon some assumptions regarding the peak absolute magnitude of supernovae, estimates of the detectable event rate as a function of γ -ray telescope sensitivity can be made. Vigorous ground-based programs that search, discover, classify, and catalog supernovae are essential prerequisites in studying the γ -ray emission in detail and, hence, studying the explosion in detail.

Data on more than 1000 extragalactic supernovae are given in the Sternberg Astronomical Institute Supernova Catalogue² and the Asiago Supernova Catalogue.³ About 50% of the supernovae in either catalog lack or have an uncertain supernova type identification; but certainly the brightest and more recent events do have supernova types assigned. All Type Ia events are assumed to have a peak absolute bolometric magnitude of $M = -19.0$. This standard candle assumption may be challenged on both observational (see, e.g., Saha et al. 1996) and theoretical (see, e.g., Höflich et al. 1996) grounds, but it remains a useful first approximation. Distances to individual supernovae are then calculated from the cataloged magnitudes by the standard formula $\log_{10} D = (m - M + 5)/5$, with no reddening corrections applied.

² Tsvetkov, Pavlyuk, & Bartunov 1997; www.sai.msu.su/groups/sn.

³ Cappellaro, Barbon, & Turatto 1997; www.pd.astro.it/supern.

All the various Type Ia models tend to produce peak 847 keV line fluxes in the $2\text{--}10 \times 10^{-5}$ photons $\text{cm}^{-2} \text{s}^{-1}$ range at $D_p = 10$ Mpc, reaching this maximum ~ 75 days after the explosion (Chan & Lingenfelter 1991; Khokhlov, Müller, & Höflich 1993; see Fig. 11). The peak 1.238 MeV line flux is slightly smaller at the same distance (due to a smaller branching ratio), and tends to lie in the $1.5\text{--}6 \times 10^{-5}$ photons $\text{cm}^{-2} \text{s}^{-1}$ range. Here we simply assume all Type Ia supernovae have a peak γ -ray flux of $F_p = 3 \times 10^{-5}$ photons $\text{cm}^{-2} \text{s}^{-1}$ at $D_p = 10$ Mpc. Peak γ -ray fluxes are then calculated by the flux ratio $F = F_p(D_p/D)^2$. Catalog completeness, volumes sampled, and limitations of the assumptions are important concerns. These are discussed in detail by Timmes & Woosley (1997), who also report a similar analysis for core-collapse supernovae.

A total of 90 Type Ia supernovae brighter than 16th apparent magnitude are listed in these catalogs (Fig. 15). As long-term search, discovery, and classification programs continue to mature, the significance of average detection and classification rate being roughly constant ($\sim 5 \text{ yr}^{-1}$ for a 16th apparent magnitude cut) may be evaluated. These implied rates are lower bounds for several reasons; a large visual extinction by dust from the parent galaxy may hide events, search programs are becoming more efficient, and unclassified events may include some Type Ia supernovae.

The apparent magnitude distribution for the 81 events discovered and identified as Type Ia supernova since 1966 are shown with the gray-scale histogram and right y-axis in Figure 15. Also shown are the six brightest Type Ia supernovae that occurred within this time span. The apparent magnitudes may be converted into distances and peak γ -ray flux values (see top and bottom ordinates) by making the standard candle assumptions described above. Integrating the histogram and normalizing to the time frames' average Type Ia supernova rate gives the γ -ray event rate as a function of the γ -ray line flux. This can be compared with instrumental sensitivities. For example, a next-generation instrument such as the proposed ATHENA mission, which has a flux sensitivity of $\sim 2 \times 10^{-6}$ photons $\text{cm}^{-2} \text{s}^{-1}$ to 5000 km s^{-1} broadened lines, should easily observe Type Ia events in the Virgo (18.2 Mpc), Fornax (18.4 Mpc), and possibly the Hydra (41 Mpc) galaxy clusters at a rate of 1 yr^{-1} (roughly 10%–30% of all Type Ia events within 100 Mpc). The transparency of galaxies to γ -rays may allow γ -ray telescopes that possess sufficient sensitivity to provide a direct measure of absolute supernova rates. *INTEGRAL*'s spectrometer sensitivity of $\sim 6 \times 10^{-6}$ photons $\text{cm}^{-2} \text{s}^{-1}$ (Winkler 1995), for a 10 day observation, could detect all Type Ia supernovae out to ~ 20 Mpc and allow a rate near 1 Type Ia event yr^{-1} . Instrument with broad line flux sensitivities larger than 1.5×10^{-5} photons $\text{cm}^{-2} \text{s}^{-1}$, such as present-day instruments, are probably limited to detecting Type Ia supernovae within ~ 10 Mpc. These numbers indicate the minimum sensitivity for detection. Actually studying the emission in detail so as to learn, e.g., about the physics of the explosion by the velocity structure and velocity distribution of the ^{56}Ni γ -

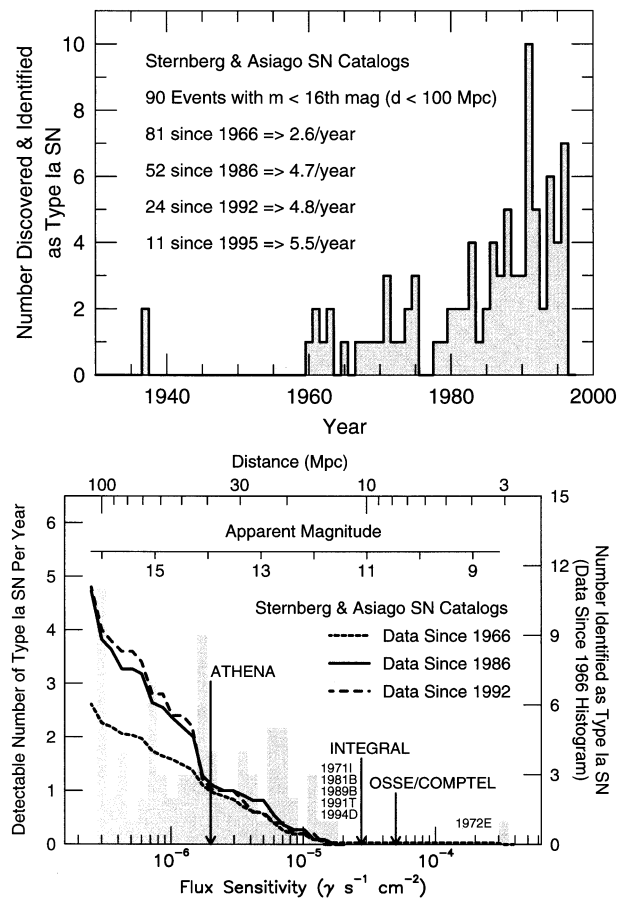


FIG. 15.—*Top*: Number of events discovered and identified as Type Ia supernovae vs. the year of the explosion. *Bottom*: Gamma-ray flux sensitivity of 1966–1996 Type Ia events (adapted from Timmes & Woosley 1997).

ray lines, will take considerably more sensitivity. These rate estimates should be regarded as lower bound guidelines, to aid, for example, in the design of future instruments.

6. CONCLUDING REMARKS

The search for an overarching paradigm that encompasses measurements of γ -ray emission from radioactive isotopes, the solar abundances, isotopic abundance measurements of presolar meteoritic grain, stellar nucleosynthesis calculations, and Galactic chemical evolution has seen some major advances during the last decade. Data obtained with the *CGRO* and ion microprobes in meteoritic analyses have provided key steps on this journey. Yet, our search remains unfulfilled. Our goal is noble: to explain the origin of every isotope in every location (and time) in the universe. The next few steps toward this goal include accurate determination of the Galactic ^{26}Al and ^{60}Fe masses, finding the exceptional events that eject ^{44}Ti , ^{60}Fe , ^7Be , and ^{22}Na , and putting the connection with the yields of these isotopes from stellar nucleosynthesis on solid ground. New instrumentation, analysis methods, and theoretical advances,

with their often conflicting constraints, will yield exciting adventures in these future studies.

Useful discussions with many colleagues are reflected in this article, in particular Don Clayton, Claes Fransson, Dieter Hartmann, Rob Hoffman, Peter Höflich, Mark Leising, Richard

Lingenfelter, Juan Naya, Nikos Prantzos, Reuven Ramaty, Stan Woosley, and Ernst Zinner. This work has been supported by the Max Planck Gesellschaft (R. D.), the National Science Foundation under grant PHY94-07194 to the Institute for Theoretical Physics at UC Santa Barbara (R. D. and F. X. T.), and a *Compton Gamma Ray Observatory* Postdoctoral Fellowship (F. X. T.).

REFERENCES

- Ahmad, I., et al. 1998, *Phys. Rev. Lett.*, in press
- Allen, S. J. 1911, *Phys. Rev.*, 34, 296
- Anders, E., & Zinner, E. 1993, *Meteoritics*, 28, 490
- Arnett, W. D. 1977, *Ann. NY Acad. Sci.*, 302, 90
- Arnett, W. D., Bahcall, J. N., Kirshner, R. P., & Woosley, S. E. 1989, *ARA&A*, 27, 629
- Arnould, M., Paulus, G., & Meynet, G. 1997, *A&A*, 321, 452
- Aufderheide, M., Baron, E., & Thielemann, F.-K. 1991, *ApJ*, 370, 630
- Badash, L. B. 1979, *Radioactivity in America: Growth and Decay of a Science* (Baltimore: Johns Hopkins Univ. Press)
- Bazan, G., & Arnett, D. 1994, *ApJ*, 433, L41
- Becquerel, H. 1896, *Compt. Rend.*, 122, 420
- . 1900, *Compt. Rend.*, 130, 809
- Birck, J. L., & Lugmair, G. W. 1988, *Earth Planet. Sci. Lett.*, 90, 131
- Blake, J. B., & Dearborn, D. S. P. 1989, *ApJ*, 338, L17
- Boffin, H. M. J., Paulus, G., Arnould, M., & Mowlavi, N. 1993, *A&A*, 279, 173
- Borkowski, K. J., Szymkowiak, A. E., Blondin, J. M., & Sarazin, C. L. 1996, *ApJ*, 466, 866
- Bouchet, P., & Danziger, I. J. 1993, *A&A*, 273, 451
- Braun, H., & Langer, N. 1995, *A&A*, 297, 483
- Brown, B. L., Leventhal, M., & Mills, A. P., Jr. 1986, *Phys. Rev. A*, 33, 2281
- Brown, L. E., & Clayton, D. D. 1992, *Science*, 258, 970
- Burbidge, E. M., Burbidge, G. R., Fowler, W. A., & Hoyle, F. 1957, *Rev. Mod. Phys.*, 29, 547
- Burrows, A., Hayes, J., & Fryxell, B. A. 1995, *ApJ*, 450, 830
- Bussard, R. W., Ramaty, R., & Drachman, R. J. 1979, *ApJ*, 228, 928
- Cameron, A. G. W. 1957, *Chalk River Report*, CRL-41
- . 1993, in *Protostars and Planets III*, ed. E. H. Levy & J. Lunine (Tucson: Univ. Arizona Press), 47
- Chan, K., & Lingenfelter, R. 1991, *ApJ*, 368, 515
- Chen, W., et al. 1997, in *The Transparent Universe: Proc. Second INTEGRAL Workshop*, ed. C. Winkler, T. J.-L. Courvoisier, & P. Durouchoux (ESA SP-382), 105
- Clayton, D. D. 1971, *Nature*, 234, 291
- . 1982, in *Essays in Nuclear Astrophysics*, ed. C. A. Barnes, D. D. Clayton, & D. N. Schramm (Cambridge: Cambridge Univ. Press), 401
- Clayton, D. D., Colgate, S. A., & Fishman, G. 1969, *ApJ*, 220, 353
- Clayton, D. D., & Leising, M. D. 1987, *Phys. Rep.*, 144, 1
- Clayton, D. D., Leising, M. D., The, L.-S., Johnson, W. N., & Kurfess, J. D. 1992, *ApJ*, 399, L141
- Coc, A., Mochkovitch, R., Oberto, Y., Thibaud, J.-P., & Vangioni-Flam, E. 1995, *A&A*, 299, 479
- Compton, A. H. 1929, *Naturwissenschaften*, 17, 507
- Dame, T. M., et al. 1987, *ApJ*, 322, 706
- del Rio, E., et al. 1996, *A&A*, 315, 237
- Diehl, R., et al. 1995, *A&A*, 298, 445
- . 1998, in *AIP Conf. Proc. 410, Fourth Compton Symp. on Gamma-Ray Astronomy and Astrophysics*, ed. C. Dermer, J. Kurfess, & M. Strickman (New York: AIP), 1109
- Dupraz, C., et al. 1997, *A&A*, in press
- Dwek, E., Moseley, S. H., Glaccum, W., Graham, J. R., Loewenstein, R. F., Silverberg, R. F., & Smith, R. K. 1992, *ApJ*, 389, 21
- Ellison, D. C., et al. 1994, *PASP*, 106, 780
- Elmegreen, B., G., & Efremov, Y. N. 1996, *ApJ*, 466, 802
- Feather, N. 1973, *Lord Rutherford* (London: Priory Press)
- Fesen, R. A., & Becker, R. H. 1991, *ApJ*, 371, 621
- Fransson, C., & Kozma, C. 1993, *ApJ*, 408, L25
- . 1998, in *The Fifth CTIO/ESO/LCO Workshop, SN 1987A: Ten Years After*, ed. M. M. Phillips & N. B. Suntzeff (San Francisco: ASP), in press
- Gallino, R., Busso, M., Picchio, G., & Raiteri, C. M. 1990, *Nature*, 348, 298
- Gehrels, N., & Chen, W. 1996, *A&AS*, 120, 331
- Gehrels, N., Fichtel, C. E., Fishman, G. J., Kurfess, J. D., & Schönfelder, V. 1993, *Sci. Am.*, 269, 68
- Glanz, J. 1997, *Science*, 276, 1789
- Glasner, S. A., Livne, E., & Truran, J. W. 1997, 475, 754
- Görres, J., et al. 1998, *Phys. Rev. Lett.*, in press
- Grabelsky, D. A., Cohen, R. S., Bronfman, L., Thaddeus, P., & May, J. 1987, *ApJ*, 315, 122
- Harper, C. E. 1996, *ApJ*, 466, 1026
- Harris, M. J. 1998, in *AIP Conf. Proc. 410, Fourth Compton Symp. on Gamma-Ray Astronomy and Astrophysics*, ed. C. Dermer, J. Kurfess, & M. Strickman (New York: AIP), 1079
- Harris, M. J., Leising, M. D., & Share, G. H. 1991, *ApJ*, 375, 216
- Hartmann, D. H., et al. 1997, *Nucl. Phys. A*, 621, 83
- Haymes, R. C., Walraven, G. D., Meegan, C. A., Hall, R. D., Djuth, F. T., & Shelton, D. H. 1975, *ApJ*, 201, 593
- Hernanz, M., José, J., Coc, A., & Isern, J. 1996, *ApJ*, 465, L27
- Higdon, J. C., & Fowler, W. A. 1987, *ApJ*, 317, 750
- Hix, W. R., & Thielemann, F. K. 1996, *ApJ*, 460, 869
- Hoffman, R. D., Woosley, S. E., Weaver, T. A., Timmes, F. X., Eastman, R. G., & Hartmann, D. H. 1995, in *The Gamma-Ray Sky with Compton GRO and SIGMA*, ed. M. Signore, P. Salati, & G. Vedrenne (Dordrecht: Kluwer), 267
- Höflich, P., Khokhlov, A., Wheeler, J. C., Phillips, M. M., Suntzeff, N. B., & Hamuy, M. 1996, *ApJ*, 472, 81
- Holt, S. S., Gotthelf, E. V., Tsunemi, H., & Negoro, H. 1994, *PASJ*, 46, L151
- Hoppe, P., Strebler, R., Eberhardt, P., Amari, S., & Lewis, R. S. 1996, *Science*, 272, 1314
- Hoyle, F., & Clayton, D. D. 1974, *ApJ*, 191, 705
- Iben, I., Jr., & Livio, M. 1993, *PASP*, 105, 1373
- Iyudin, A. F. 1997, in *Proc. Second INTEGRAL Workshop, The Transparent Universe*, ed. C. Winkler, T. J.-L. Courvoisier, & P. Durouchoux (ESA SP-382), 37
- Iyudin, A. F., et al. 1994, *A&A*, 284, L1
- Iyudin, A. F., et al. 1995, *A&A*, 300, 422
- Iyudin, A. F., et al. 1997, in *The Transparent Universe*, ed. C. Winkler, T. J.-L. Courvoisier, & P. Durouchoux (ESA SP-382) (Noordwijk: ESA), 39

- Johnson, W. N. III, Harnden, F. R., Jr., & Haymes, R. C. 1972, *ApJ*, 172, L1
- José, J., & Hernanz, M. 1998, *ApJ*, 494, 680
- José, J., Hernanz, M., & Coc, A. 1997, *ApJ*, 479, L55
- Kessler, M. F., et al. 1996, *A&A*, 315, L27
- Khokhlov, A., Müller, E., & Höflich, P. 1993, *A&A*, 270, 223
- Kinzer, R. L., Purcell, W. R., Johnson, W. N., Kurfess, J. D., Jung, G., & Skibo, J. 1996, *A&AS*, 120, 317
- Kniffen, D. A., Gehrels, N., & Fishman, G. 1998, in *AIP Conf. Proc. 410, Fourth Compton Symp. on Gamma-Ray Astronomy and Astrophysics*, ed. C. Dermer, J. Kurfess, & M. Strickman (New York: AIP), 524
- Knödlseeder, J. 1998, Ph.D. thesis, CESR/UPS, Toulouse, France
- Knödlseeder, J., Bennett, K., Bloemen, H., Diehl, R., Hermsen, W., Oberlack, U., Ryan, J., & Schönfelder, V. 1996a, *A&AS*, 120, 327
- Knödlseeder, J., et al. 1998, in *Lecture Notes in Physics 506, The Local Bubble and Beyond*, ed. D. Breitschwerdt, Mj. Freyberg, & J. Trümper (IAU Collq. 166) (Berlin: Springer), 389
- Knödlseeder, J., et al. 1996b, *A&AS*, 120, 335
- Kolb, U., & Politano, M. 1997, *A&A*, 319, 909
- Kurfess, J. D., et al. 1992, *ApJ*, 399, L137
- Kurfess, J. D., et al. 1998, *Low/Medium Energy Gamma-Ray Astrophysics Mission Workshop*, internal report
- Lagage, P. O., Claret, A., Ballet, J., Boulanger, F., Cesarsky, C. J., Cesarsky, D., Fransson, C., Pollock, A. 1996, *A&A*, 315, L273
- Langer, N., Fliegner, J., Heger, A., & Woosley, S. E. 1997, *Nucl. Phys. A*, 621, 183
- Lee, T., Papanastassiou, D. A., & Wasserburg, G. J. 1977, *ApJ*, 211, L107
- Leising, M. D. 1993, *A&AS*, 97, 299
- Leising, M. D., & Clayton, D. D. 1987, *ApJ*, 323, 159
- Leising, M. D., et al. 1995, *ApJ*, 450, 805
- Leising, M. D., & Share, G. H. 1994, *ApJ*, 424, 200
- Lewis, R. S., Amari, S., & Anders, E. 1993, *Geochim. Cosmochim. Acta*, 289, 970
- Lichti, G. G., et al. 1994, *A&A*, 292, 569
- Lingenfelter, R. E., Chan, K. W., & Ramaty, R. 1993, *Phys. Rep.*, 227, 133
- Lingenfelter, R. E., & Ramaty, R. 1978, *Phys. Today*, 31, 40
- . 1989, *ApJ*, 343, 686
- Livne, E., & Arnett, D. 1995, *ApJ*, 452, 62
- Livne, E., & Glasner, A. S. 1991, *ApJ*, 370, 272
- Lyne, A. G., & Lorrimer, D. R. 1994, *Nature*, 369, 127
- MacPherson, G. J., Davis, A. M., & Zinner, E. K. 1995, *Meteoritics*, 30, 365
- Mahoney, W. A., Ling, J. C., Jacobson, A. S., & Lingenfelter, R. E. 1982, *ApJ*, 262, 742
- Mahoney, W. A., Ling, J. C., Wheaton, W. A., & Higdon, J. C. 1992, *ApJ*, 387, 314
- Meynet, G., & Maeder, A. 1997, *A&A*, 321, 465
- Meynet, G., Arnould, M., Prantzos, N., & Paulus, G. 1997, *A&A*, 320, 460
- Mezzacappa, A., Calder, A. C., Bruenn, S. W., Blondin, J. M., Guidry, M. W., Strayer, M. R., & Umar, A. S. 1998, *ApJ*, 493, 848
- Morfill, G. E., & Hartquist, T. W. 1985, *ApJ*, 297, 194
- Morris, D. J., Bennet, K., Bloemen, H., Hermsen, W., Lichti, G., McConnell, M. L., Ryan, J. M., & Schönfelder, V. 1995, *Proc. 17th Texas Symp. on Rel. Astrophys. and Cosm.*, ed. H. Böhringer, G. E. Morfill, & J. E. Trümper (NY Acad. Sci., Vol. 759), 397
- . 1998, in *AIP Conf. Proc. 410, Fourth Compton Symp. on Gamma-Ray Astronomy and Astrophysics*, ed. C. Dermer, J. Kurfess, & M. Strickman (New York: AIP), 1084
- Murthy, P. V. R., & Wolfendale, A. W. 1993, *Gamma-Ray Astronomy* (Cambridge: Cambridge Univ. Press)
- Myra, E. S., & Burrows, A. 1990, *ApJ*, 364, 222
- Naya, J. E., Barthelmy, S. D., Bartlett, L. M., Gehrels, N., Leventhal, M., Parsons, A., Teegarden, B. J., & Tueller, J. 1996, *Nature*, 384, 44
- Naya, J., Barthelmy, S. D., Gehrels, N., Parsons, A., Teegarden, B., Tueller, J., & Leventhal, M. 1998, in *ApJ*, in press
- Nagataki, S., Hashimoto, M., Sato, K., & Yamada, S. 1997, *ApJ*, 486, 1026
- Nichols, R. H., Jr., Amari, S., Hohenberg, C. M., Hoppe, P., & Lewis, R. S. 1993, *Meteoritics*, 428, 410
- Nittler, L. R., Amari, S., Zinner, E., Woosley, S. E., & Lewis, R. S. 1996, *ApJ*, 462, L31
- Norman, E. B., et al. 1998, in *Second Oak Ridge Symp. on Atomic and Nuclear Astrophysics*, ed. A. Mezzacappa (Bristol: IOP), in press
- Oberlack, U. 1998, Ph.D. thesis, Tech. Univ., München
- Oberlack, U., et al. 1994, *ApJS*, 92, 433
- Ott, U. 1993, *Nature*, 364, 25
- Pöppel, W. 1997, *Fund. Cosmic Phys.*, 18, 1
- Politano, M., Starrfield, S., Truran, J. W., Weiss, A., & Sparks, W. M. 1995, *ApJ*, 448, 807
- Prantzos, N. 1993a, *ApJ*, 405, L55
- . 1993b, *A&A*, 97, 119
- Prantzos, N., & Diehl, R. 1996, *Phys. Rep.*, 267, 1
- Predehl, P., & Schmitt, J. H. M. M. 1995, *A&A*, 293, 889
- Ramaty, R., & Lingenfelter, R. E. 1977, *ApJ*, 213, L5
- . 1995, in *The Analysis of Emission Lines: A Meeting in Honor of the 70th Birthdays of D. E. Osterbrock & M. J. Seaton* (Cambridge: Cambridge Univ. Press), 180
- Ramaty, R., Skibo, J. G., & Lingenfelter, R. E. 1994, *ApJS*, 92, 393
- Ritossa, C., Garcia-Berro, E., & Iben, I., Jr. 1996, *ApJ*, 460, 489
- Rolfs, C. E., & Rodney, W. S. 1988, *Cauldrons in the Cosmos* (Chicago: Univ. Chicago Press)
- Rona, E. 1978, *How It Came About: Radioactivity, Nuclear Physics, Atomic Energy* (Oak Ridge: Oak Ridge Associated Univ.)
- Rothschild, R. E., et al. 1997, in *AIP Conf. Proc. 410, Fourth Compton Symp. on Gamma-Ray Astronomy and Astrophysics*, ed. C. Dermer, J. Kurfess, & M. Strickman (New York: AIP), 1089
- Rutherford, E. 1899, *Phil. Mag.*, 47, 109
- . 1905, *Radio-activity* (Cambridge: Cambridge Univ. Press)
- . 1919, *Phil. Mag.*, 37, 581
- Saha, A., Sandage, A., Labhardt, L., Tammann, G. A., Macchetto, F. D., & Panagia, N. 1996, *ApJS*, 107, 693
- Schaerer, D., Schmutz, W., & Grenon, M. 1997, *ApJ*, 484, L153
- Schönfelder, V., et al. 1996, *A&AS*, 120, 13
- Shankar, A., & Arnett, D. 1994, *ApJ*, 433, 216
- Shigeyama, T., Kumagai, S., Yamaoka, H., Nomoto, K., & Thielemann, F. K. 1993, *A&AS*, 97, 223
- Shu, F. H., Shang, H., Lee, T., Glassgold, A. E. 1997, *BAAS*, 190, 4904
- Shukolyukov, A., & Lugmair, G. W. 1993, *Science*, 259, 1138
- Simpson, J. A., & Connell, J. J. 1998, *ApJ*, 487, L85
- Smith, D. M., Purcell, W. R., & Leventhal, M. 1998, in *AIP Conf. Proc. 410, Fourth Compton Symp. on Gamma-Ray Astronomy and Astrophysics*, ed. C. Dermer, J. Kurfess, & M. Strickman (New York: AIP), 28
- Starrfield, S., et al. 1996, in *ASP Conf. Ser. 99, Cosmic Abundances*, ed. S. S. Holt & G. Sonneborn (San Francisco: ASP), 242
- Starrfield, S., Shore, S. N., Sparks, W. M., Sonneborn, G., Truran, J. W., & Politano, M. 1992, *ApJ*, 391, 71
- Starrfield, S., Truran, J. W., Politano, M., Sparks, W. M., Nofar, I., & Shaviv, G. 1993, *Phys. Rep.*, 227, 223

- Suntzeff, N. B. 1998, in *The Fifth CTIO/ESO/LCO Workshop, SN 1987A: Ten Years After*, ed. M. M. Phillips & N. B. Suntzeff (San Francisco: ASP), in press
- Suntzeff, N. B., Phillips, M. M., Elias, J. H., Walker, A. R., & Depoy, D. L. 1992, *ApJ*, 384, L33
- Tammann, G. A., Löffler, W., & Schröder, A. 1994, *ApJS*, 92, 487
- Taylor, J. H., & Cordes, J. M. 1993, *ApJ*, 411, 674
- The, L. S., et al. 1995, *ApJ*, 444, 244
- The, L. S., Leising, M. D., Kurfess, J. D., Johnson, W. N., Hartmann, D. H., Gehrels, N., Grove, J. E., & Purcell, W. R. 1996, *A&AS*, 120, 357
- Thielemann, F.-K., Nomoto, K., & Hashimoto, M. A. 1996, *ApJ*, 460, 408
- Thielemann, F.-K., Nomoto, K., & Yokoi, Y. 1986, *A&A*, 158, 17
- Timmes, F. X., Diehl, R., & Hartmann, D. H. 1997, *ApJ*, 479, 760
- Timmes, F. X., & Woosley, S. E. 1997, *ApJ*, 489, 160
- Timmes, F. X., Woosley, S. E., Hartmann, D. H., Hoffman, R. D., Weaver, T. A., & Matteucci, F. 1995, *ApJ*, 449, 204
- Timmes, F. X., Woosley, S. E., Hoffman, R. D., & Hartmann, D. H. 1996a, *ApJ*, 464, 332
- Timmes, F. X., Woosley, S. E., & Weaver, T. A. 1996b, *ApJ*, 457, 834
- Tutukov, A. V., Yungelson, L. R., & Iben, I., Jr. 1992, *ApJ*, 386, 197
- van den Bergh, S., & McClure, R. D. 1994, *ApJ*, 425, 205
- van den Bergh, S., & Pritchett, C. J. 1986, *ApJ*, 307, 723
- van der Hucht, K. A., Hidayat, B., Admiranto, A. G., Supelli, K. R., & Doom, C. 1988, *A&A*, 199, 217
- van der Hucht, K. A., et al. 1997, *NewA*, 2, 245
- Wasserburg, G. J., Gallino, R., Busso, M., & Raiteri, C. M. 1995, *ApJ*, 440, L101
- Weiss, A., & Truran, J. W. 1990, *A&A*, 238, 178
- Williams, B. F., Schmitt, M. D., & Winkler, P. F. 1995, *BAAS*, 186, 4911
- Winkler, C. 1995, *Exp. Astron.*, 6, 71
- Winkler, C., et al. 1997, in *The Transparent Universe: Proc. Second INTEGRAL Workshop*, ed. C. Winkler, T. J.-L. Courvoisier, & P. Durouchoux (ESA SP-382), 105
- Woosley, S. E., Arnett, W. D., & Clayton, D. D. 1973, *ApJS*, 26, 231
- Woosley, S. E., Hartmann, D. H., Hoffman, R. D., & Haxton, W. C. 1990, *ApJ*, 356, 272
- Woosley, S. E., Langer, N., & Weaver, T. A. 1995, *ApJ*, 448, 315
- Woosley, S. E., Pinto, P. A., & Hartmann, D. H. 1989, *ApJ*, 346, 395
- Woosley, S. E., & Timmes, F. X. 1996, *Nucl. Phys. A*, 606, 137
- Woosley, S. E., & Weaver, T. A. 1994, *ApJ*, 423, 371
- . 1995, *ApJS*, 101, 181
- Zinner, E. 1997, in *Astrophysical Implications of the Laboratory Study of Presolar Materials*, ed. T. J. Bernatowicz & E. Zinner (New York: AIP), 3